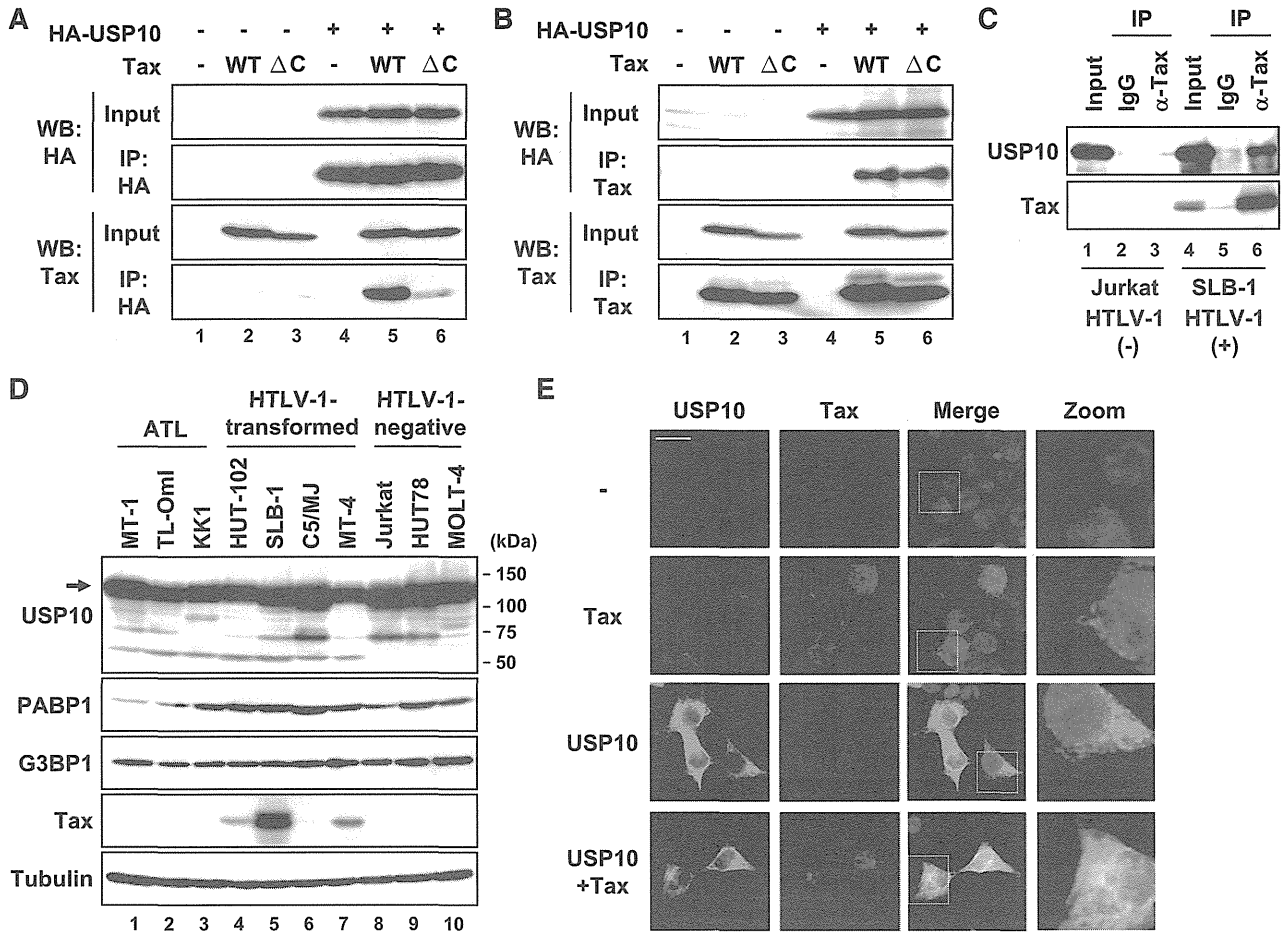

Figure 1. Tax interacts with USP10. (A,B) 293T cells were transfected with a control plasmid (lanes 1, 4), Tax plasmid (lanes 2, 5), or TaxΔC plasmid (lanes 3, 6) together with (lanes 4-6) or without (lanes 1-3) an HA-USP10 plasmid. At 48 hours after transfection, the cell lysates were immunoprecipitated with anti-HA (A) or anti-Tax (B) antibodies, and the total lysates (input) and immunoprecipitates (IP) were characterized using a western blot analysis with anti-HA and anti-Tax antibodies. TaxΔC has a 4 amino acid deletion on the Tax C-terminus, the peptide of which is missing in the nonleukemogenic HTLV-2 Tax2, because the original goal was to isolate binding factors specific to Tax but not to Tax2. (C) The cell lysates prepared from HTLV-1–uninfected T cells (Jurkat; lanes 1-3) and HTLV-1–infected T cells (SLB-1; lanes 4-6) were immunoprecipitated with anti-Tax antibodies (lanes 3, 6) or control antibodies (lanes 2, 5). The input lysate and IP were characterized using a western blot analysis with anti-USP10 and anti-Tax antibodies. (D) Cell lysates were prepared from 7 HTLV-1–infected T-cell lines (lanes 1-7) and 3 HTLV-1–uninfected T-cell lines (lanes 8-10). The expressions of USP10, PABP1, G3BP1, Tax, and α-tubulin proteins were determined using a western blot analysis with the corresponding antibodies. (E) 293T cells were transfected with a Tax plasmid together with or without the HA-USP10 plasmid. The transfected cells were stained with anti-USP10 (green) and anti-Tax (red) antibodies. The nuclei were counterstained with Hoechst33258 (blue). The bar indicates 20 μm.

deletion of amino acids 1 to 116 of the *N*-terminal region, which are essential for the formation of SGs as well as binding with G3BP1 and PABP1,[3] had a minimal effect on binding with Tax (Figure 2D), indicating that Tax interacts with amino acids 727 to 798 of USP10.

Binding of Tax with USP10 inhibits arsenite-induced SG formation

USP10 is a component of SGs that is involved in innate immunity against viral infections.[8] Intriguingly, Tax inhibits SG formation.[14] Therefore, we next investigated whether USP10 is involved in the Tax-mediated inhibition of SG formation. Arsenite, a prooxidant well known to stimulate SG formation, induced SGs in 293T cells, and USP10 was predominantly detected in the formed SGs (Figure 3A). The 293T cells were then transiently transfected with expression vectors encoding WT Tax, $Tax^{62\text{-}353}$, TaxSH-1, or TaxSH-2, treated with arsenite and stained with anti-USP10 antibodies. WT Tax inhibited arsenite-induced SG formation (as represented by the arrow in Figure 3B). This is consistent with the findings of a previous study.[14] In addition, 2 Tax mutants (TaxM22 and Tax703) that are capable of interacting with USP10 also reduced arsenite-induced SG formation (Figure 3D). Of the 3 Tax mutants defective in USP10 binding, $Tax^{62\text{-}353}$ was completely unable to interfere with SG formation. In contrast, the other 2 Tax mutants (TaxSH-1 and TaxSH-2) inhibited SG formation; however, the inhibitory activity was half that of WT Tax (Figure 3B-C). These results suggest that Tax inhibits SG formation and that this inhibition is partly mediated through the interaction between Tax and USP10.

Tax augments arsenite-induced apoptosis of 293T cells

Because SGs inhibit arsenite-induced apoptosis,[3,22,23] we next examined whether Tax affects the sensitivity of 293T cells to arsenite-induced apoptosis. 293T cells were transfected with expression vectors encoding Tax and its mutants, and the cells were treated with 0.5 mM of arsenite for 80 minutes, washed with PBS, and further cultured for 1 hour. The cells were then stained with anti-Tax antibodies and Hoechst33258 (supplemental Figure 1). The apoptotic cells were monitored by detecting condensed nuclei in the

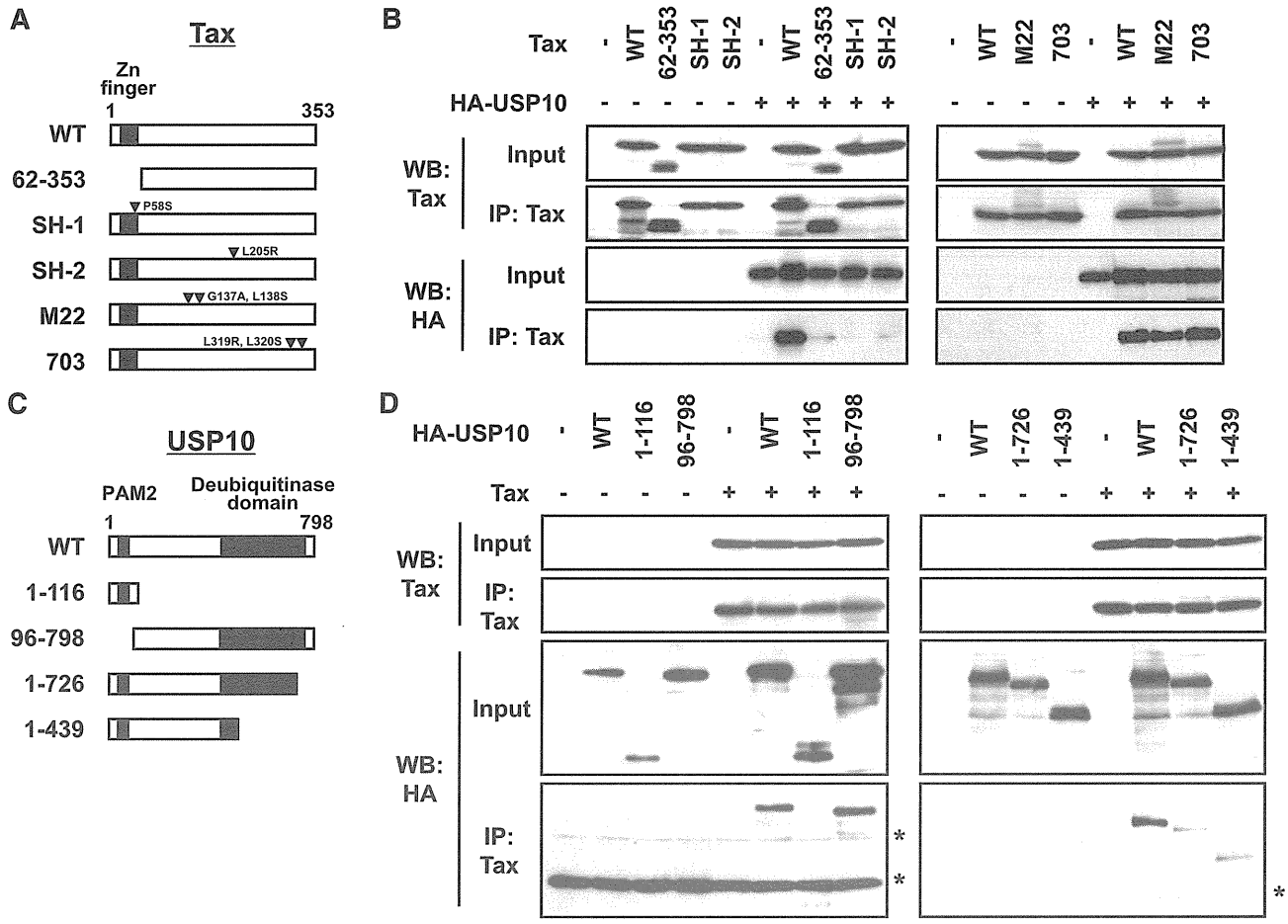

Figure 2. The domains of Tax and USP10 are required for the interaction. (A) A schematic representation of Tax and its mutants used in this study. (B) Cell lysates were prepared from 293T cells transfected with the HA-USP10 plasmid together with Tax mutant plasmids, and then were immunoprecipitated with anti-Tax. The total lysates (input) and immunoprecipitates (IP) were characterized using a western blot analysis with anti-Tax and anti-HA antibodies. (C) A schematic representation of USP10 and its mutants used in this study. PAM2 (PABP-interacting motif 2) mediates the interaction with PABP.[21] (D) 293T cells were transfected with plasmids encoding HA-tagged USP10 (HA-WT) or its mutants (HA-1-116, HA-96-798, HA-1-726, or HA-1-439), as described in (C), together with Tax plasmids. Cell lysates prepared from 293T cells were then immunoprecipitated with anti-Tax antibodies. The input and immunoprecipitates were characterized using a western blot analysis with anti-Tax and anti-HA antibodies. The asterisks indicate nonspecific bands.

Tax-expressing cells (Figure 3E). Tax augmented the arsenite-induced apoptosis of 293T cells, and this apoptosis was inhibited by an antioxidant (NAC) (Figure 3F). On the other hand, the augmentation of apoptosis induced by TaxSH-1 and TaxSH-2 in the 293T cells was approximately half that induced by WT Tax, and $Tax^{62\text{-}353}$ had a minimal effect on apoptosis (Figure 3E). These results suggest that Tax, at least in part through its interaction with USP10, augments arsenite-induced apoptosis of 293T cells, and that this apoptosis augmentation correlates with the SG inhibitory activity.

Tax stimulates ROS production via USP10 in T cells

We recently showed that USP10 downregulates steady-state ROS production in several epithelial cell lines and inhibits arsenite-induced ROS production.[3] To elucidate the role of USP10 in ROS production in T cells, we knocked down the USP10 expression in a human T-cell line (Jurkat) using short hairpin RNA (shRNA) (Figure 4A) and measured the ROS levels using staining with CM-H_2DCFDA, a redox-sensitive probe (Figure 4B). Two USP10-knockdown cells targeting different regions of *USP10* messenger RNA produced more ROS than the control cells (Figure 4C). These results suggest that endogenous USP10 in T cells downregulates ROS production under steady-state conditions.

Tax stimulates ROS production in T cells.[24] To examine whether USP10 is involved in Tax-induced ROS production in T cells, USP10-knockdown (sh-USP10-1) Jurkat and control cells (sh-NT) were infected with Tax-encoding lentivirus, and the cells were assessed for ROS production. Tax elevated ROS production in the control cells; however, this activity was abrogated by the knockdown of USP10 (Figure 4D). Two Tax mutants, TaxSH-1 and TaxSH-2, defective for USP10 interactions were unable to elevate ROS production (Figure 4D). In addition, 2 other Tax mutants (TaxM22 and Tax703) that are active for USP10 binding failed to elevate ROS production (Figure 4E). Whereas WT Tax activates the transcription of cellular genes through 2 transcription factors, NF-κB and CREB, TaxM22 is inactive for NF-κB–dependent transcriptional activation, and Tax703 exhibits a weak degree of CREB-dependent activation.[25,26] Therefore, these results suggest that transcriptional activation of cellular genes by Tax is required for the production of ROS induced by Tax. In addition, TaxΔC without PBM did not stimulate ROS production (Figure 4F). Therefore, PBM and its binding proteins are also required for Tax to stimulate ROS production. It should be noted that TaxSH-1 defective for the USP10 interaction possesses PBM and activates CREB- and NF-κB–dependent transcription equivalent to WT Tax. Taken together, these results indicate that Tax stimulates ROS production through combined

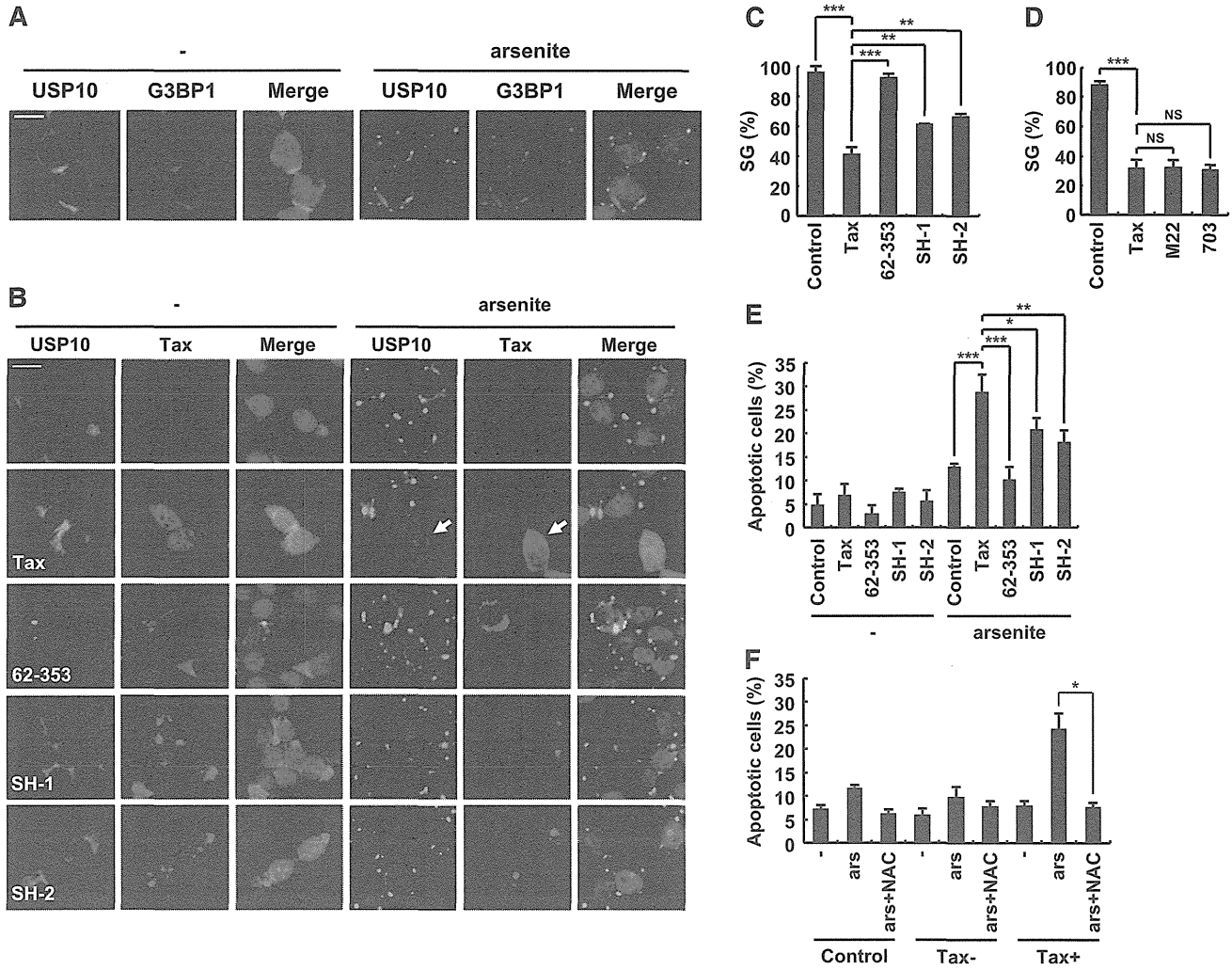

Figure 3. Tax inhibits SG formation and augments arsenite-induced apoptosis. (A) 293T cells were treated with 0.5 mM of sodium arsenite for 60 minutes and then were stained with anti-USP10 antibodies (green), anti-G3BP1 antibodies (red), and Hoechst33258 (blue). The bar indicates 20 μm. (B) 293T cells were transfected with the indicated plasmids (Tax, $Tax^{62\text{-}353}$, TaxSH-1, or TaxSH-2). The transfected cells were treated with 0.5 mM of sodium arsenite for 60 minutes and then were stained with anti-USP10 antibodies (green), anti-Tax (red) antibodies, and Hoechst33258 (blue). The arrow indicates a cell that exhibits reduced SG formation. The bar indicates 20 μm. (C,D) The SG (%) in Tax-positive cells and control cells is presented. (E) The number of cells containing condensed nuclei among the Tax-positive cells was counted. (F) 293T cells were transfected with Tax plasmids and then were incubated with or without 5 mM of NAC, treated with 0.5 mM of sodium arsenite, and stained with anti-Tax antibodies and Hoechst33258. The numbers of cells containing condensed nuclei among the Tax-positive cells and the control cells were counted. In all experiments, the values denote mean ± SD; $^*P < .05$; $^{**}P < .01$; $^{***}P < .001$; NS indicates not statistically significant.

actions by interacting with USP10 and modulating the activities of the NF-κB, CREB, and PBM pathways.

USP10 knockdown in T cells reduces SG-forming activities and augments sensitivity to arsenite-induced apoptosis

We next investigated the roles of USP10 in arsenite-induced SG formation and apoptosis in T cells. High-dose arsenite (0.25 mM) induced SG formation in 2 distinct USP10-knockdown Jurkat cells; however, the level of SGs was less than that observed in the control cells (Figure 5A-B). In addition, knockdown of USP10 augmented the apoptosis of Jurkat cells treated with or without a low dose of arsenite (5 μM) (Figure 5C). It should be noted that human T-cell lines are more sensitive to arsenite-induced apoptosis than adherent cell lines, including 293T cells, and even a concentration of arsenite (5 μM) that does not induce the formation of visible SGs can still induce apoptosis in T-cell lines, but not adherent cell lines. These results indicate that USP10 in T cells augments SG formation and reduces arsenite-induced apoptosis.

Augmented arsenite-induced apoptosis of HTLV-1–infected T cells is associated with a reduced level of SG-forming activity

A recent study showed that combination therapy containing arsenic trioxide, interferon-α, and zidovudine exhibits promising therapeutic effects on some forms of ATL.[16] In addition, arsenite induces apoptosis in HTLV-1–infected T-cell lines more so than in HTLV-1–uninfected T-cell lines.[27] Therefore, we next examined whether the high sensitivity of HTLV-1–infected T-cell lines to arsenite is related to the level of SG-forming activity. HTLV-1–infected T-cell lines treated with a low dose of arsenite exhibited more apoptosis than the HTLV-1–uninfected cell lines (Figure 6C). This apoptosis was inhibited by NAC (Figure 6D). In addition, high-dose arsenite induced SG formation in HTLV-1–infected T-cell lines, and the amount of SGs was lower than that observed in the HTLV-1–uninfected cell lines (Figure 6A-B). Moreover, USP10 knockdown in the HTLV-1–infected T-cell line MT-4 induced less arsenite-induced SG formation, more ROS production, and more arsenite-induced apoptosis than the control USP10-competent MT-4

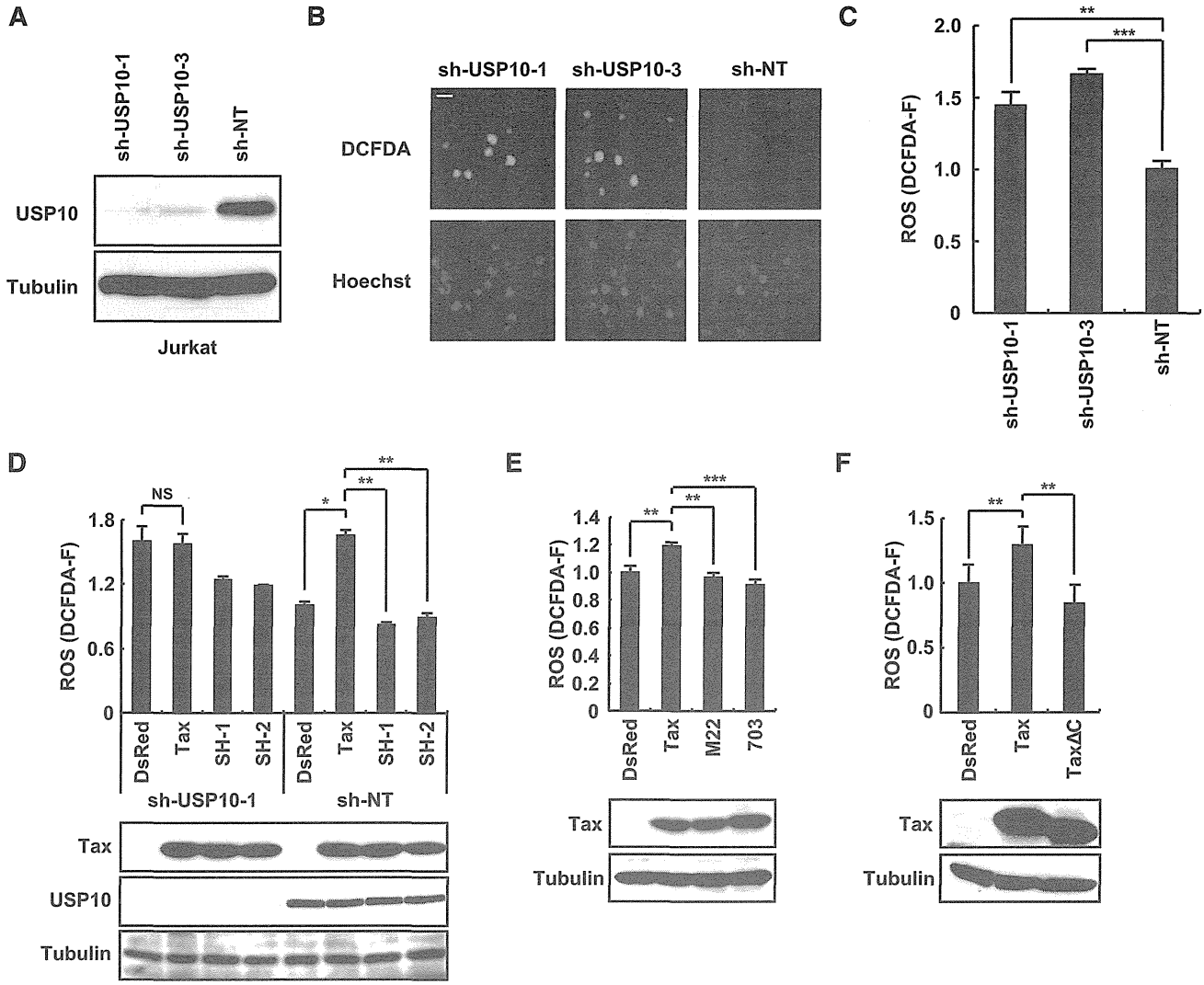

Figure 4. Tax stimulates ROS production in part through an interaction with USP10. (A) Jurkat cells were infected with lentiviruses encoding human *USP10* shRNA (sh-USP10-1 or sh-USP10-3) or control nontargeting shRNA (sh-NT), and the cells were then cultured in the presence of puromycin. Cell lysates prepared from the selected cells were characterized using a western blot analysis with anti-USP10 and anti-α-tubulin antibodies. (B) USP10-knockdown Jurkat cells and control cells were stained with 5 μM of CM-H_2DCFDA (green) and Hoechst33258 (blue) for 5 minutes at 37°C. Staining of the cells was visualized using a fluorescence microscope. The bar indicates 10 μm. (C) The ROS levels (DCFDA-F) in cells treated as in (B) were quantitatively measured using a cell imaging software program. (D-F) USP10-knockdown (sh-USP10-1) Jurkat cells and control (sh-NT) (D) or Jurkat cells (E,F) were infected with the indicated Tax lentiviruses. The infected cells were assessed for ROS production (DCFDA-F) using 5 μM of CM-H_2DCFDA. Aliquots of the above-treated cells were subjected to a western blot analysis using anti-Tax, anti-USP10, and anti-α-tubulin antibodies. In all experiments, the values denote the mean ± SD; $^*P < .05$; $^{**}P < .01$; $^{***}P < .001$; NS indicates not statistically significant.

cells (supplemental Figure 2). Collectively, these results indicate that USP10 inhibits ROS production and apoptosis in HTLV-1–infected T cells and that the inhibition correlates with the SG-forming activity.

Arsenic trioxide, an anhydrous form of arsenite, has been used as a drug against ATL in place of sodium arsenite.[28] To confirm that arsenic trioxide also exhibits similar activities to arsenite, we treated HTLV-1–uninfected (Jurkat) and infected (SLB-1) T-cell lines with arsenic trioxide. Arsenic trioxide (0.1-1.0 mM) induced SG formation in both the Jurkat and SLB-1 cells; however, the level of SG-forming activity was lower in the SLB-1 cells than in the Jurkat cells (supplemental Figure 3A). Moreover, the arsenic trioxide-induced apoptosis of the SLB-1 cells was significantly greater than that of the Jurkat cells, and the apoptosis was abrogated by treatment with NAC (supplemental Figure 3B-C). These results suggest that arsenic trioxide induces the ROS-dependent apoptosis of HTLV-1–infected T cells via the same mechanism as sodium arsenite (Figure 6).

Approximately half of leukemic cells in patients with ATL do not express a functional *tax* gene.[29] Therefore, we next examined whether 3 ATL cell lines established from patients with ATL are sensitive to arsenite-induced apoptosis. Three ATL cell lines with or without a minimal amount of a Tax protein expression demonstrated different sensitivities to arsenite-induced apoptosis, and the level of sensitivity correlated inversely with the level of SG-forming activity (Figure 7A-B). These results suggest that sensitivity to arsenite-induced apoptosis in ATL cells is also regulated by SG-forming activities. To extend this hypothesis into cell types other than T cells, we characterized the sensitivity to arsenite-induced apoptosis and the SG-forming activity of leukemia/lymphoma cell lines unrelated to ATL. The 3 B-cell lines (Ramos, Daudi, and BJAB) were derived from Burkitt lymphoma (Figure 7C-D); the next one (NB4), from promyeloid leukemia; and the last one (THP-1), from acute monocytic leukemia (Figure 7E-F). They exhibited distinct sensitivities to arsenite-induced apoptosis, and the level of sensitivity correlated

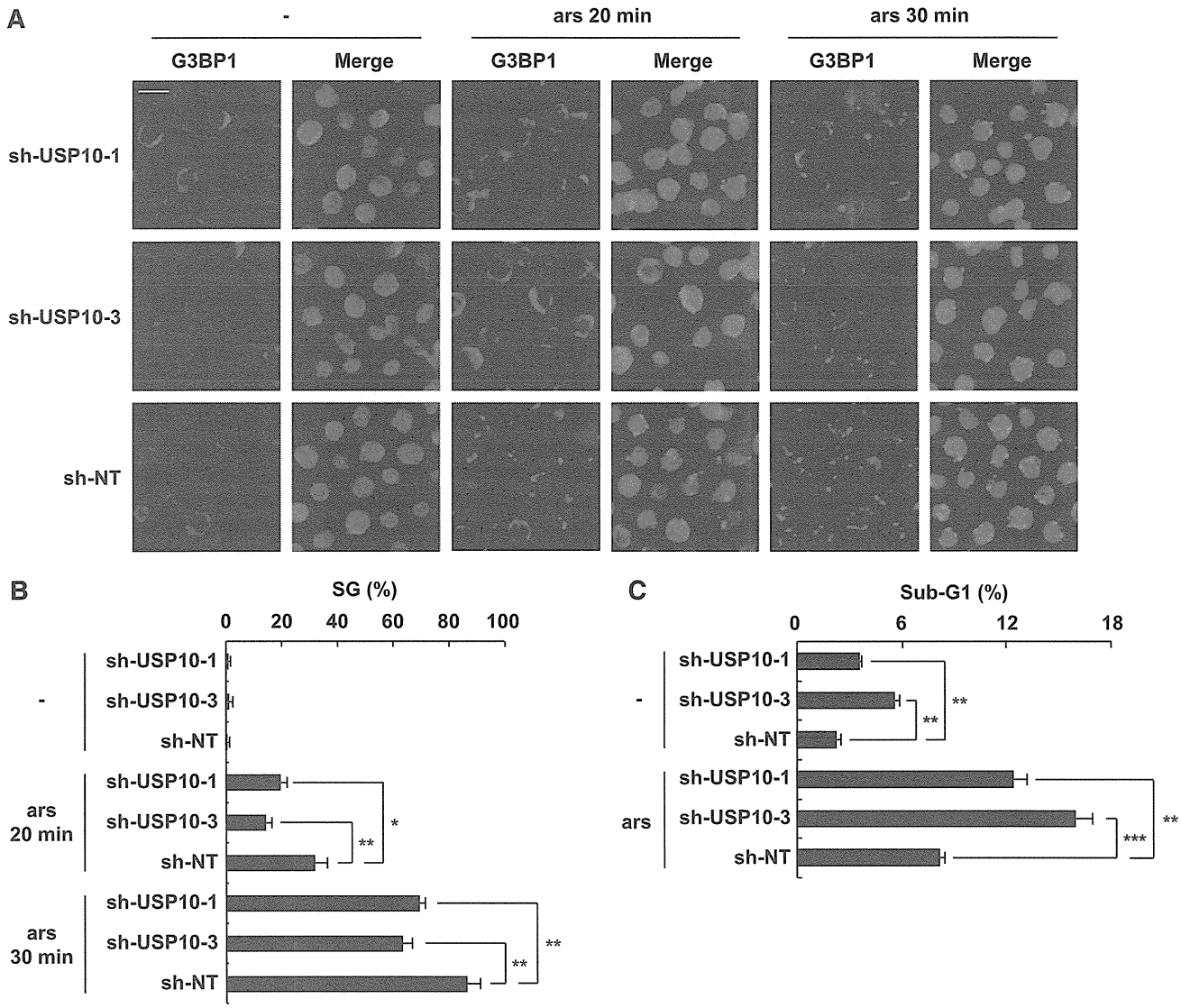

Figure 5. USP10 in T cells controls the SG-forming activity and sensitivity to arsenite-induced apoptosis. (A) USP10-knockdown Jurkat cells and control cells were treated with 0.25 mM of sodium arsenite for 0, 20, and 30 minutes and then were stained with anti-G3BP1 antibodies (red) and Hoechst33258 (blue). The bars indicate 10 μm. (B) The SG (%) is presented. (C) USP10-knockdown Jurkat cells and control cells were treated with 5 μM of sodium arsenite for 48 hours and then were stained with propidium iodide (PI). The proportion of the sub-G1 fraction was measured using flow cytometry. In all experiments, the values denote the mean ± SD; $*P < .05$; $**P < .01$; $***P < .001$.

inversely with the level of SG-forming activity. These results further support the idea that arsenite-induced SG formation of various hematopoietic leukemic cells correlates inversely with sensitivity to arsenite-induced apoptosis.

Discussion

In our study, we identified USP10 as a novel binding protein of HTLV-1 Tax in T cells and found that Tax inhibits at least 3 USP10-associated functions, namely, SG formation, ROS suppression, and inhibition of apoptosis. Under various stress conditions, including viral infection, USP10 can prevent the emergence of cells with stress-induced ROS-dependent DNA and protein alterations.[3] Therefore, our present findings suggest that Tax, by interacting with USP10, augments ROS-dependent alterations, such as DNA damage, in HTLV-1–infected T cells, thereby promoting leukemogenesis.

Two Tax mutants (TaxSH-1 and TaxSH-2) defective for USP10 binding inhibited SG formation; however, the inhibition achieved by these mutants was half that of WT Tax. Legros et al demonstrated that Tax inhibits SG formation by binding to histone deacetylase 6 (HDAC6), a component of SGs.[14] Therefore, both USP10 and HDAC6 are likely to play a role in the Tax-induced inhibition of SG formation. On the other hand, HDAC6 is not likely to mediate Tax-induced ROS production because, unlike WT Tax, TaxSH-1 and TaxSH-2 have a minimal effect on ROS production.

The activities of the Tax mutants suggest that multiple functions of Tax, in addition to the inhibition of USP10 functions, are involved in the stimulation of ROS production. Two Tax mutants (TaxM22 and Tax703), which are defective for NF-κB- and CREB-dependent transcriptional activation, respectively, both failed to elevate ROS production (Figure 4), suggesting that Tax stimulates ROS generation via gene(s) regulated by NF-κB and CREB. Indeed, NF-κB can

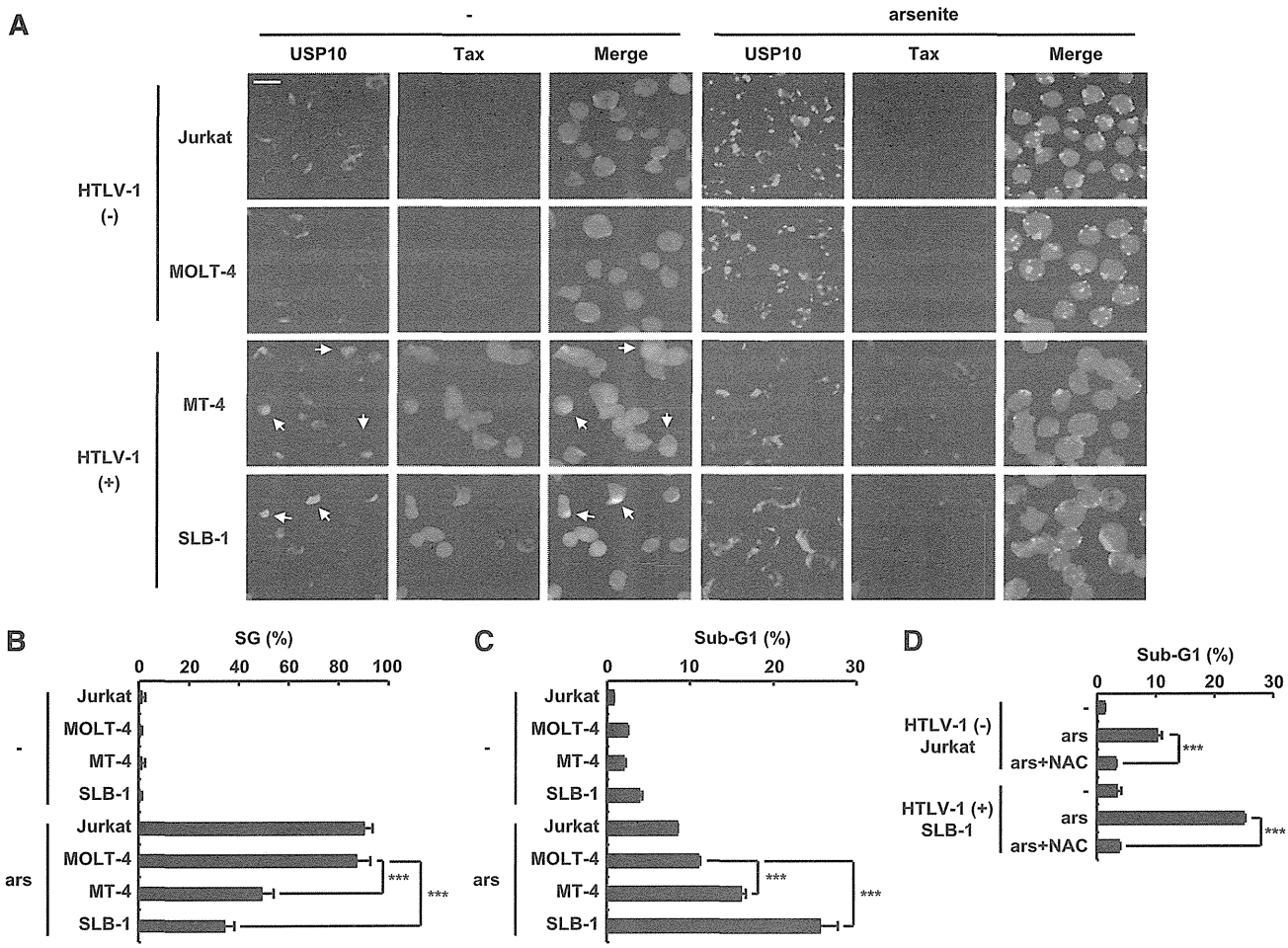

Figure 6. The level of arsenite sensitivity of HTLV-1–infected T cells correlates with the level of SG-forming activity. (A,B) HTLV-1–uninfected (Jurkat and MOLT-4) and HTLV-1–infected (SLB-1 and MT-4) T cells were treated with 0.5 mM of sodium arsenite for 30 minutes and then were stained with anti-USP10 antibodies (green), anti-Tax antibodies (red), and Hoechst33258 (blue). The arrows indicate cells with colocalization of USP10 and Tax. The bar indicates 10 μm in (A). The SG (%) in the indicated cells is presented in (B). (C) HTLV-1–uninfected (Jurkat and MOLT-4) and HTLV-1–infected (MT-4 and SLB-1) T cells were treated with 5 μM of sodium arsenite for 48 hours and then were stained with PI. The proportion of the sub-G1 population (apoptotic cells) was measured using flow cytometry. (D) Jurkat and SLB-1 cells were incubated with or without 10 mM of NAC, further treated with 5 μM of sodium arsenite for 48 hours, and stained with PI. The proportion of sub-G1 populations (%) was measured using flow cytometry. In all experiments, the values denote mean ± SD; $^{***}P < .001$.

activate prooxidant genes, such as the reduced NAD phosphate oxidase NOX2.[30,31] In addition, PBM was required for Tax to stimulate ROS production (Figure 4). Tax, acting through PBM, interacts with several PDZ domains containing proteins, including Dlg1, Scribble, and MAGI-1, then inactivates the functions of these PDZ proteins by altering subcellular localization.[32-35] The PDZ proteins localize near the plasma membrane and form a complex with several membrane receptors, then positively or negatively control signals from corresponding membrane receptors.[36,37] Collectively, we tentatively propose the following hypothesis of how Tax stimulates ROS production in T cells. Although Tax, acting through the NF-κB, CREB, and PBM pathways, induces the expression of prooxidant gene(s), by acting through USP10, it blocks the antioxidant response, thereby prolonging the production of ROS. A further analysis is, however, required to understand the precise mechanisms underlying how Tax stimulates ROS production in T cells.

Tax is an ubiquitinated protein, and the ubiquitination controls the stability and transcriptional activity of Tax.[38,39] Although USP10 is a Tax-interacting deubiquitinase, the overexpression of USP10 in 293T cells minimally affects the ubiquitination of Tax (H.M, M.T., and M.F., unpublished observations). In this aspect, several proteins have been shown to modulate the ubiquitination of Tax. For instance, USP20 directly deubiquitinates Tax and suppresses the NF-κB activation induced by Tax.[40] In addition, the metalloprotease STAM-binding protein-like 1 indirectly induces the deubiquitination of Tax, thereby stabilizing Tax and promoting its nuclear export.[41] On the other hand, Tax is ubiquitinated by The Really Interesting New Gene Finger Protein 4, and this ubiquitination is required for cytoplasmic localization and the activation of NF-κB.[42] Therefore, further analyses of these cellular proteins, including USP10, will clarify the precise mechanisms underlying the functions of Tax in the pathogenesis of HTLV-1.

A previous study showed that USP10 inhibits arsenite-induced ROS-dependent apoptosis in MEFs and that this inhibitory activity is mediated by the formation of USP10-containing SGs.[3] In our study, unlike MEFs, USP10 inhibited arsenite-induced ROS-dependent apoptosis in a human T-cell line, even at a concentration of arsenite that does not provoke visible SG formation. These results suggest 2 possible mechanisms. USP10 may block ROS-dependent apoptosis without forming SGs in T cells. Alternatively, a low concentration of arsenite may induce small SGs undetectable

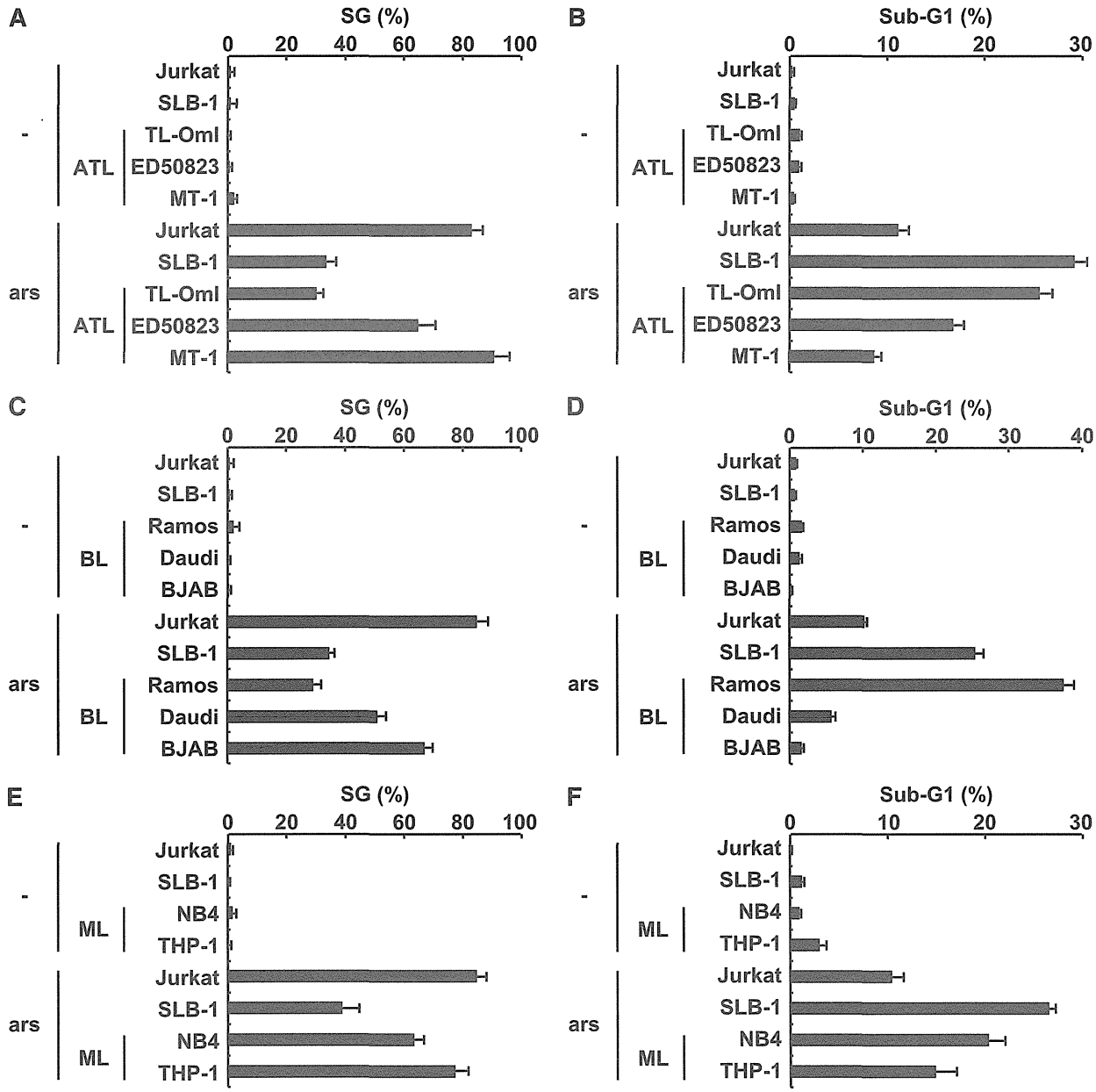

Figure 7. The level of sensitivity to arsenite-induced apoptosis in ATL, Burkitt lymphoma, and myeloid leukemia cell lines correlates with the level of SG-forming activity. (A) HTLV-1–uninfected (Jurkat), HTLV-1–infected (SLB-1; used as a positive control), and ATL-derived (TL-Oml, ED50823, and MT-1) T-cell lines were treated with 0.5 mM of sodium arsenite for 30 minutes and then were stained with anti-USP10 antibodies and Hoechst33258. The SG (%) is presented. (B) HTLV-1–uninfected (Jurkat), HTLV-1–infected (SLB-1), and ATL-derived (TL-Oml, ED50823, and MT-1) T-cell lines were treated with 5 μM of sodium arsenite for 48 hours and then were stained with PI. The proportion of the sub-G1 population (%) (apoptotic cells) was measured using flow cytometry. (C-F) The levels of arsenite-induced SG formation (%) and the proportions of the sub-G1 population (%) in the Burkitt lymphoma (C,D) and myeloid leukemia (ML) cell lines (E,F) were assessed.

by the present assay method, and such undetectable small SGs may inhibit apoptosis. We are currently studying how USP10 inhibits arsenite-induced apoptosis without visible SGs in T cells.

A clinical trial has indicated that combination therapy containing arsenic trioxide, interferon α, and zidovudine exhibits promising antileukemia activity against some forms of ATL[16]; however, it is unclear which patients are sensitive to this chemotherapy. Our present study suggests that Tax augments the sensitivity to arsenite-induced apoptosis of cells. Takeda et al showed that 66% of ATL cells exhibit inactivation of the *tax* gene because of mutation or DNA methylation.[29] Therefore, the expression of the *tax* gene in ATL cells is likely to be a factor controlling the sensitivity of ATL cells to chemotherapy containing arsenic. In addition, a single ATL-derived cell line without a Tax expression (TL-OmI) demonstrated higher sensitivity to arsenite-induced apoptosis than the other 2 ATL cell lines (Figure 7), and the different levels of arsenite sensitivity correlated with the level of SG-forming activity in the cells. Therefore, factor(s) other than Tax control(s) the sensitivity of ATL cells to arsenite-induced apoptosis, and this sensitivity might also be related to the SG-forming activity. Because the SG-forming activity is regulated by various host factors, such as G3BP1,[6] G3BP2,[43] and HDAC6,[22] these host proteins may be involved in the high arsenite-induced apoptosis of ATL cell lines without a Tax expression.

Arsenic trioxide is a highly effective chemotherapy for promyelocytic leukemia (PML).[28] Arsenic trioxide induces ROS-dependent apoptosis in several PML cell lines, including NB4, in vitro.[44,45] In our study, in addition to ATL cell lines, 5 leukemia cell lines derived from PML, myeloid leukemia, and Burkitt lymphoma exhibited distinct sensitivities to arsenite-induced apoptosis, and the level of sensitivity correlated with the degree of arsenite-induced SG formation. Therefore, understanding how USP10 and SGs control sensitivity to arsenite-induced apoptosis in hematopoietic cells will provide useful information for developing more effective chemotherapies for the treatment of hematopoietic malignancies, including ATL.

Acknowledgments

The authors thank Dr H. Miyoshi (RIKEN Tsukuba Institute, Japan) for providing the lentiviral packaging plasmids and Dr M. Masuko (Niigata University, Japan) for providing NB4 cells. The authors also thank the Takeda Pharmaceutical Company for providing recombinant human IL-2 and M. Tobimatsu for technical assistance.

This work was supported in part by a Grant-in-aid from the Ministry of Education, Culture, Sports, Science and Technology of Japan and by a Grant for the Promotion of Niigata University Research Project.

Authorship

Contribution: M.T. performed most of the experiments and contributed to the data interpretation; M.H. performed the mass spectrometry analysis and contributed to the data interpretation; G.N.M., H.M., and M.Y. assisted in conducting the experiments; Y.T. provided the anti-Tax antibody; and M.F. contributed to the conception, design, and data interpretation of the study and wrote and drafted the manuscript.

Conflict-of-interest disclosure: The authors declare no competing financial interests.

Correspondence: Masahiro Fujii, Division of Virology, Niigata University Graduate School of Medical and Dental Sciences, Niigata 951-8510, Japan; e-mail: fujiimas@med.niigata-u.ac.jp.

References

1. Anderson P, Kedersha N. RNA granules: post-transcriptional and epigenetic modulators of gene expression. *Nat Rev Mol Cell Biol.* 2009;10(6):430-436.
2. Buchan JR, Parker R. Eukaryotic stress granules: the ins and outs of translation. *Mol Cell.* 2009;36(6):932-941.
3. Takahashi M, Higuchi M, Matsuki H, et al. Stress granules inhibit apoptosis by reducing reactive oxygen species production. *Mol Cell Biol.* 2013;33(4):815-829.
4. White JP, Lloyd RE. Regulation of stress granules in virus systems. *Trends Microbiol.* 2012;20(4):175-183.
5. White JP, Cardenas AM, Marissen WE, Lloyd RE. Inhibition of cytoplasmic mRNA stress granule formation by a viral proteinase. *Cell Host Microbe.* 2007;2(5):295-305.
6. Tourrière H, Chebli K, Zekri L, et al. The RasGAP-associated endoribonuclease G3BP assembles stress granules. *J Cell Biol.* 2003;160(6):823-831.
7. Khaperskyy DA, Hatchette TF, McCormick C. Influenza A virus inhibits cytoplasmic stress granule formation. *FASEB J.* 2012;26(4):1629-1639.
8. Beckham CJ, Parker R. P bodies, stress granules, and viral life cycles. *Cell Host Microbe.* 2008;3(4):206-212.
9. Matsuoka M, Jeang KT. Human T-cell leukemia virus type 1 (HTLV-1) and leukemic transformation: viral infectivity, Tax, HBZ and therapy. *Oncogene.* 2011;30(12):1379-1389.
10. Chlichlia K, Khazaie K. HTLV-1 Tax: Linking transformation, DNA damage and apoptotic T-cell death. *Chem Biol Interact.* 2010;188(2):359-365.
11. Grassmann R, Aboud M, Jeang KT. Molecular mechanisms of cellular transformation by HTLV-1 Tax. *Oncogene.* 2005;24(39):5976-5985.
12. Boxus M, Twizere JC, Legros S, et al. The HTLV-1 Tax interactome. *Retrovirology.* 2008;5:76. doi: 10.1186/1742-4690-5-76.
13. Currer R, Van Duyne R, Jaworski E, et al. HTLV tax: a fascinating multifunctional co-regulator of viral and cellular pathways. *Front Microbiol.* 2012;3:406. doi: 10.3389/fmicb.2012.00406. Epub 2012 Nov 30.
14. Legros S, Boxus M, Gatot JS, et al. The HTLV-1 Tax protein inhibits formation of stress granules by interacting with histone deacetylase 6. *Oncogene.* 2011;30(38):4050-4062.
15. Benhar M, Engelberg D, Levitzki A. ROS, stress-activated kinases and stress signaling in cancer. *EMBO Rep.* 2002;3(5):420-425.
16. Kchour G, Tarhini M, Kooshyar MM, et al. Phase 2 study of the efficacy and safety of the combination of arsenic trioxide, interferon alpha, and zidovudine in newly diagnosed chronic adult T-cell leukemia/lymphoma (ATL). *Blood.* 2009;113(26):6528-6532.
17. Tanaka Y, Yoshida A, Tozawa H, Shida H, Nyunoya H, Shimotohno K. Production of a recombinant human T-cell leukemia virus type-I trans-activator (tax1) antigen and its utilization for generation of monoclonal antibodies against various epitopes on the tax1 antigen. *Int J Cancer.* 1991;48(4):623-630.
18. Tsubata C, Higuchi M, Takahashi M, et al. PDZ domain-binding motif of human T-cell leukemia virus type 1 Tax oncoprotein is essential for the interleukin 2 independent growth induction of a T-cell line. *Retrovirology.* 2005;2:46.
19. Higuchi M, Tsubata C, Kondo R, et al. Cooperation of NF-kappaB2/p100 activation and the PDZ domain binding motif signal in human T-cell leukemia virus type 1 (HTLV-1) Tax1 but not HTLV-2 Tax2 is crucial for interleukin-2-independent growth transformation of a T-cell line. *J Virol.* 2007;81(21):11900-11907.
20. Soncini C, Berdo I, Draetta G. Ras-GAP SH3 domain binding protein (G3BP) is a modulator of USP10, a novel human ubiquitin specific protease. *Oncogene.* 2001;20(29):3869-3879.
21. Albrecht M, Lengauer T. Survey on the PABC recognition motif PAM2. *Biochem Biophys Res Commun.* 2004;316(1):129-138.
22. Kwon S, Zhang Y, Matthias P. The deacetylase HDAC6 is a novel critical component of stress granules involved in the stress response. *Genes Dev.* 2007;21(24):3381-3394.
23. Arimoto K, Fukuda H, Imajoh-Ohmi S, Saito H, Takekawa M. Formation of stress granules inhibits apoptosis by suppressing stress-responsive MAPK pathways. *Nat Cell Biol.* 2008;10(11):1324-1332.
24. Kinjo T, Ham-Terhune J, Peloponese JM Jr, Jeang KT. Induction of reactive oxygen species by human T-cell leukemia virus type 1 tax correlates with DNA damage and expression of cellular senescence marker. *J Virol.* 2010;84(10):5431-5437.
25. Smith MR, Greene WC. Identification of HTLV-I tax trans-activator mutants exhibiting novel transcriptional phenotypes. *Genes Dev.* 1990;4(11):1875-1885.
26. Akagi T, Ono H, Nyunoya H, Shimotohno K. Characterization of peripheral blood T-lymphocytes transduced with HTLV-I Tax mutants with different trans-activating phenotypes. *Oncogene.* 1997;14(17):2071-2078.
27. Che XF, Zheng CL, Owatari S, et al. Overexpression of survivin in primary ATL cells and sodium arsenite induces apoptosis by down-regulating survivin expression in ATL cell lines. *Blood.* 2006;107(12):4880-4887.
28. Dilda PJ, Hogg PJ. Arsenical-based cancer drugs. *Cancer Treat Rev.* 2007;33(6):542-564.
29. Takeda S, Maeda M, Morikawa S, et al. Genetic and epigenetic inactivation of tax gene in adult T-cell leukemia cells. *Int J Cancer.* 2004;109(4):559-567.
30. Morgan MJ, Liu ZG. Crosstalk of reactive oxygen species and NF-κB signaling. *Cell Res.* 2011;21(1):103-115.
31. Anrather J, Racchumi G, Iadecola C. NF-kappaB regulates phagocytic NADPH oxidase by inducing the expression of gp91phox. *J Biol Chem.* 2006;281(9):5657-5667.
32. Suzuki T, Ohsugi Y, Uchida-Toita M, Akiyama T, Yoshida M. Tax oncoprotein of HTLV-1 binds to the human homologue of Drosophila discs large tumor suppressor protein, hDLG, and perturbs its function in cell growth control. *Oncogene.* 1999;18(44):5967-5972.
33. Arpin-André C, Mesnard JM. The PDZ domain-binding motif of the human T cell leukemia virus type 1 tax protein induces mislocalization of the tumor suppressor hScrib in T cells. *J Biol Chem.* 2007;282(45):33132-33141.
34. Okajima M, Takahashi M, Higuchi M, et al. Human T-cell leukemia virus type 1 Tax induces an aberrant clustering of the tumor suppressor Scribble through the PDZ domain-binding motif

dependent and independent interaction. *Virus Genes.* 2008;37(2):231-240.

35. Makokha GN, Takahashi M, Higuchi M, Saito S, Tanaka Y, Fujii M. Human T-cell leukemia virus type 1 Tax protein interacts with and mislocalizes the PDZ domain protein MAGI-1. *Cancer Sci.* 2013;104(3):313-320.
36. Harris BZ, Lim WA. Mechanism and role of PDZ domains in signaling complex assembly. *J Cell Sci.* 2001;114(Pt 18):3219-3231.
37. Subbaiah VK, Kranjec C, Thomas M, Banks L. PDZ domains: the building blocks regulating tumorigenesis. *Biochem J.* 2011;439(2):195-205.
38. Peloponese JM Jr, Iha H, Yedavalli VR, et al. Ubiquitination of human T-cell leukemia virus type 1 tax modulates its activity. *J Virol.* 2004;78(21): 11686-11695.
39. Nasr R, Chiari E, El-Sabban M, et al. Tax ubiquitylation and sumoylation control critical cytoplasmic and nuclear steps of NF-kappaB activation. *Blood.* 2006;107(10): 4021-4029.
40. Yasunaga J, Lin FC, Lu X, Jeang KT. Ubiquitin-specific peptidase 20 targets TRAF6 and human T cell leukemia virus type 1 tax to negatively regulate NF-kappaB signaling. *J Virol.* 2011; 85(13):6212-6219.
41. Lavorgna A, Harhaj EW. An RNA interference screen identifies the Deubiquitinase STAMBPL1 as a critical regulator of human T-cell leukemia virus type 1 tax nuclear export and NF-κB activation. *J Virol.* 2012;86(6):3357-3369.
42. Fryrear KA, Guo X, Kerscher O, Semmes OJ. The Sumo-targeted ubiquitin ligase RNF4 regulates the localization and function of the HTLV-1 oncoprotein Tax. *Blood.* 2012;119(5): 1173-1181.
43. Matsuki H, Takahashi M, Higuchi M, Makokha GN, Oie M, Fujii M. Both G3BP1 and G3BP2 contribute to stress granule formation. *Genes Cells.* 2013;18(2):135-146.
44. Chen GQ, Zhu J, Shi XG, et al. In vitro studies on cellular and molecular mechanisms of arsenic trioxide (As2O3) in the treatment of acute promyelocytic leukemia: As2O3 induces NB4 cell apoptosis with downregulation of Bcl-2 expression and modulation of PML-RAR alpha/PML proteins. *Blood.* 1996;88(3):1052-1061.
45. Jing Y, Dai J, Chalmers-Redman RM, Tatton WG, Waxman S. Arsenic trioxide selectively induces acute promyelocytic leukemia cell apoptosis via a hydrogen peroxide-dependent pathway. *Blood.* 1999;94(6):2102-2111.

Kinpara et al. Retrovirology 2013, 10:52
http://www.retrovirology.com/content/10/1/52

RETROVIROLOGY

RESEARCH Open Access

Interferon-α (IFN-α) suppresses HTLV-1 gene expression and cell cycling, while IFN-α combined with zidovudin induces p53 signaling and apoptosis in HTLV-1-infected cells

Shuichi Kinpara[1,2], Mami Kijiyama[1], Ayako Takamori[1], Atsuhiko Hasegawa[1], Amane Sasada[1], Takao Masuda[1], Yuetsu Tanaka[3], Atae Utsunomiya[4] and Mari Kannagi[1*]

Abstract

Background: Human T-cell leukemia virus type-1 (HTLV-1) is the causative retrovirus of adult T-cell leukemia/lymphoma (ATL) and HTLV-1-associated myelopathy/tropical spastic paraparesis (HAM/TSP). HTLV-1 gene expression is maintained at low levels *in vivo* by unknown mechanisms. A combination therapy of interferon-α (IFN-α) and zidovudin (AZT) shows therapeutic effects in ATL patients, although its mechanism is also obscure. We previously found that viral gene expression in IL-2-dependent HTLV-1-infected T-cells (ILTs) derived from ATL patients was markedly suppressed by stromal cells through a type I IFN response. Here, we investigated the effects of IFN-α with or without AZT on viral gene expression and cell growth in ILTs.

Results: ILTs expressed variable but lower amounts of HTLV-1 Tax protein than HTLV-1-transformed HUT102 cells. Following the addition of IFN-α, the amounts of HTLV-1 p19 in the supernatants of these cells decreased in three days, while HTLV-1 gene expression decreased only in ILTs but not HUT102 cells. IFN-α also suppressed the spontaneous HTLV-1 induction in primary ATL cells cultured for 24 h. A time course study using ILTs revealed that the levels of intracellular Tax proteins decreased in the first 24 h after addition of IFN-α, before the reduction in HTLV-1 mRNA levels. The initial decreases of Tax protein following IFN-α treatment were observed in 6 of 7 ILT lines tested, although the reduction rates varied among ILT lines. An RNA-dependent protein kinase (PKR)-inhibitor reversed IFN-mediated suppression of Tax in ILTs. IFN-α also induced cell cycle arrest at the G0/G1 phase and suppressed NF-κB activities in these cells. AZT alone did not affect HTLV-1 gene expression, cell viability or NF-κB activities. AZT combined with IFN-α markedly induced cell apoptosis associated with phosphorylation of p53 and induction of p53-responsive genes in ILTs.

Conclusions: IFN-α suppressed HTLV-1 gene expression at least through a PKR-mediated mechanism, and also induced cell cycle arrest in ILTs. In combination with AZT, IFN-α further induced p53 signaling and cell apoptosis in these cells. These findings suggest that HTLV-1-infected cells at an IL-2-dependent stage retain susceptibility to type I IFN-mediated regulation of viral expression, and partly explain how AZT/IFN-α produces therapeutic effects in ATL.

Keywords: ATL, HTLV-1, IFN-α, PKR, Innate immunity, Anti-viral therapy, AZT, p53

* Correspondence: kann.impt@tmd.ac.jp
[1]Department of Immunotherapeutics, Graduate School of Medical and Dental Sciences, Tokyo Medical and Dental University, 1-5-45 Yushima, Bunkyo-ku, Tokyo 113-8519, Japan
Full list of author information is available at the end of the article

Background

Human T-cell leukemia virus type 1 (HTLV-1) causes adult T-cell leukemia/lymphoma (ATL) [1-3], a malignant lympho-proliferative disorder resistant to chemotherapy. The virus is also responsible for HTLV-1-associated myelopathy/tropical spastic paraparesis (HAM/TSP) [4,5], a chronic inflammatory demyelinating disorder. Despite such severe clinical outcomes, levels of HTLV-1 gene expression are thought to be very low *in vivo*. HTLV-1 mRNA, but not proteins, are detectable in peripheral blood mononuclear cells (PBMCs) of HTLV-1-infected individuals [6]. Although undetectable, a low level of HTLV-1 proteins must be present *in vivo*, as HTLV-1-infected individuals maintain antibodies against HTLV-1 structural proteins and Tax protein-specific cytotoxic T lymphocytes.

Recent therapeutic approaches, such as allogeneic hematopoietic stem cell transplantation (allo-HSCT) [7,8], a humanized antibody therapy targeting CCR4 [9,10], or anti-viral therapy with interferon (IFN)-α and zidovudin (AZT) [11-13] partly improved ATL prognosis. *Ex vivo* studies have indicated that graft-versus-tumor responses including anti-Tax cytotoxic T-cells were potentially involved in the therapeutic mechanisms of allo-HSCT [14], and that the CCR4-antibodies were capable of inducing antibody-dependent cellular cytotoxicities [15]. However, combining AZT/IFN-α hardly affects HTLV-1-infected cells *in vitro* [16], and the mechanisms of its therapeutic effects remain unclear. A recent report indicated that the triple combination of arsenic trioxide/IFN-α/AZT demonstrated more favorable therapeutic effects in ATL patients [17]. The combination of arsenic trioxide and IFN-α has been reported to induce proteolysis of Tax in HTLV-1-infected cells *in vitro* [18,19]. As IFN-α is indispensable in AZT/IFN-α, arsenic trioxide/IFN-α or arsenic trioxide/IFN-α/AZT therapies, ATL cells might be susceptible to IFNs *in vivo*.

It is well established that HTLV-1-infected cells are resistant to type I IFNs *in vitro*. For example, IFN-α reduced the virus release but not viral protein synthesis in HTLV-1-transformed HUT102 or MT-2 cells [20]. The mechanisms of the resistance to type I IFNs in HTLV-1-infected cells include reduction in the phosphorylation of Tyk2 and STAT2 [21], Tax-mediated competition with CREB binding protein/p300 [22], Tax-mediated up-regulation of SOCS1 [23,24], and up-regulation of IRF4 [25], all of which result in inhibition of IFN signaling. This may explain why IFN-α combined with AZT does not affect HTLV-1-infected cells *in vitro*, while conflicting with the clinical effects of AZT/IFN-α therapy in ATL patients. This discrepancy between *in vivo* and *in vitro* systems can be partially attributed to differences in status of HTLV-1-infected cells between the two systems.

We previously found that HTLV-1-infected cells could induce type I IFN responses in co-cultured stromal cells [26]. We also found that viral expression in HTLV-1-infected T-cells is markedly suppressed at both mRNA and protein levels through type I IFN responses mediated by stromal cells co-cultured [26]. This observation again conflicts with the previous notion of HTLV-1-mediated resistance to type I IFNs *in vitro*. Our experimental system differed from previous studies in two ways. First, we used IL-2-dependent HTLV-1-infected T-cells (ILTs) derived from ATL patients, while previous studies used IL-2-independent HTLV-1-transformed cell lines such as HUT102. Second, we used stromal cells as effectors; these mediated the type I IFN response, but could have also produced multiple factors other than IFNs.

In the present study, we investigated whether purified type I-IFNs can affect viral expression and cell growth of HTLV-1-infected cells by using various ILTs. Here we report a novel finding that IFN-α suppresses intracellular Tax expression at a translational level at least through PKR. We further demonstrate that IFN-α activates p53 pathways in cooperation with AZT, partly explaining the mechanisms of the therapeutic effects of AZT/IFN-α in ATL.

Results

Effects of IFN-α on HTLV-1 p19 release and viral transcription

We evaluated the baseline levels of HTLV-1 gene expression in HUT102, ILT-Hod and ILT-#29 cell lines (Figure 1A). Relative levels of HTLV-1 mRNA in ILT-Hod and ILT-#29 cells were comparable with those in HUT102 cells. However, the levels of Tax protein in ILT-Hod and ILT-#29 cells were much lower than those of HUT102, and were barely detectable by immunoblotting only after stimulation of ILTs with phorbol 12-myristate 13-acetate (PMA). Flow cytometry results also indicated that ILT-Hod and ILT-#29 cells expressed smaller amounts of intracellular Tax protein than HUT102 cells. In addition, our analyses often identified Tax-negative cell populations in ILTs, with the ratio of these populations fluctuating during culture. These cells are also HTLV-1-infected, as all the cells in ILT-Hod and ILT-#29 cultures express HTLV-1 Gag protein after stimulation with PMA (Figure 1A insert), suggesting a dynamic turnover of HTLV-1 proteins in ILTs. Tax expression in HUT102 cells was apparently stable (Figure 1A).

We added IFN-α at various concentrations (300, 3000, and 30000 IU/ml) on HUT102, ILT-Hod, and ILT-#29 cells (Figure 1B). The amounts of HTLV-1 p19 released in supernatants significantly decreased after 72 h in culture for all the cell lines tested. Gag mRNA levels were also decreased in ILT-Hod and ILT-#29 in 3 days of culture (Figure 1B). These suppressive effects were observed at all doses of IFN-α used, indicating that 300 IU/ml of IFN-α was sufficient to produce these effects.

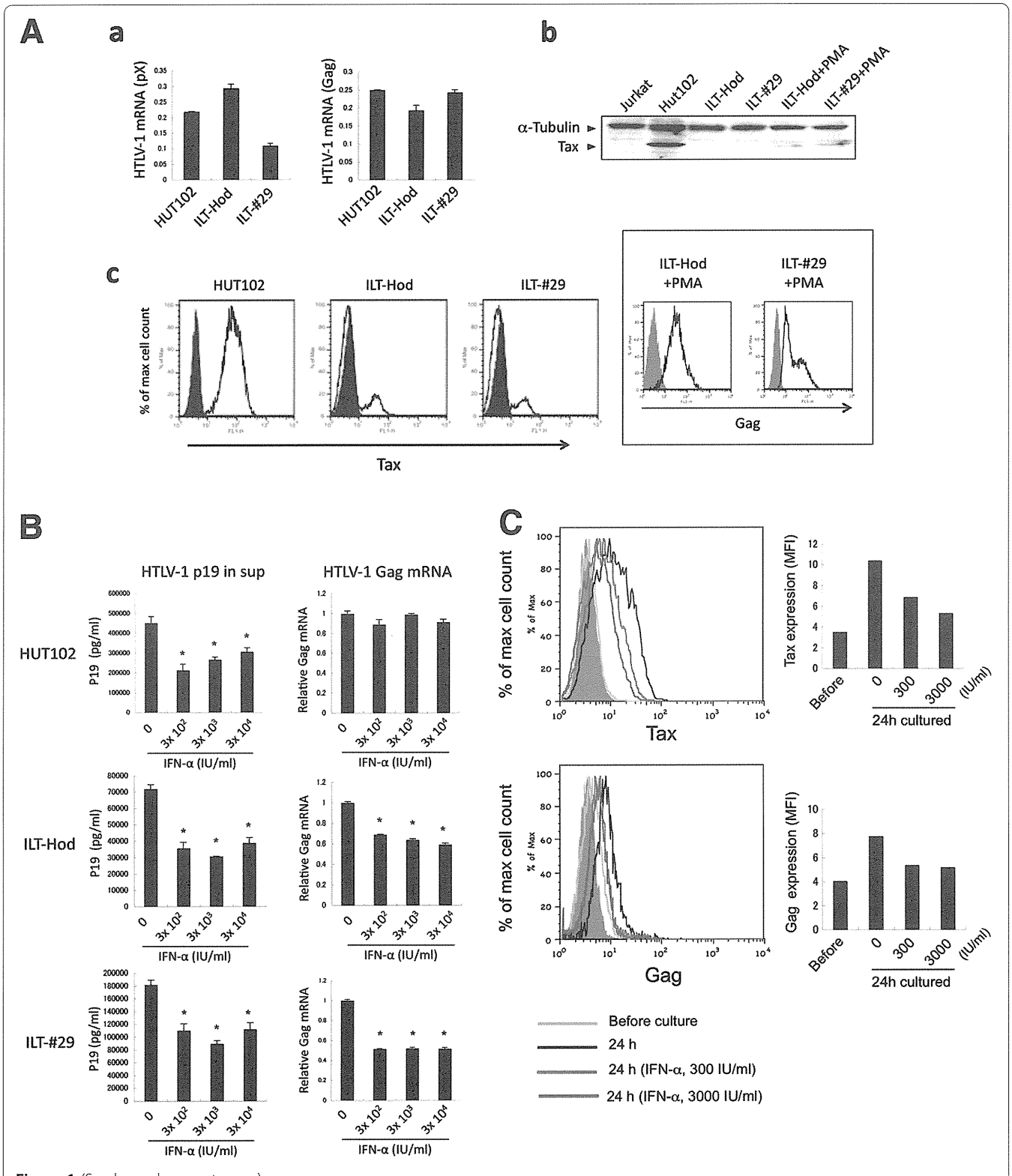

Figure 1 (See legend on next page.)

(See figure on previous page.)
Figure 1 Effects of IFN-α treatment on HTLV-1 p19 release and viral transcription in various HTLV-1-infected cell lines. A. Expression of HTLV-1 mRNAs (**a**) and proteins (**b**, **c**) were evaluated by quantitative RT-PCR (**a**), immunoblotting (**b**), and flow cytometry (**c**), respectively, in HTLV-1-infected HUT102, ILT-Hod and ILT-#29 or uninfected Jurkat cell lines. **a**. The mRNA copy numbers measured by using pX or Gag primers were standardized to those for GAPDH and indicated as the means and standard deviations (SD) of duplicate samples. **b**. Cell lysates from indicated cell lines were subjected to an immunoblotting assay with antibodies to Tax (40 kDa) and α-Tubulin (50 kDa). The lysates in lanes 5 and 6 were prepared from ILT-Hod and ILT-#29 cells stimulated with PMA (50 ng/ml) overnight, respectively. **c**. Intracellular Tax proteins in permeabilized cells were stained with Alexa Fluor 488-labeled anti-Tax mAb (open histogram) and mouse IgG3 isotype control antibody (closed histogram). The inserted box indicates Gag expression in ILT-Hod and ILT-#29 cells stimulated with PMA (50 ng/ml) for 17h. **B**. HUT102 (top), ILT-Hod (middle) and ILT-#29 (bottom) cells were cultured for 3 days with or without three doses of IFN-α indicated. HTLV-1 p19 concentrations in the supernatants (left) and Gag mRNA levels were measured by ELISA and quantitative RT-PCR, respectively. Data are presented as the means and SD of duplicate samples. **C**. Frozen stored primary ATL cells were thawed and analyzed for intracellular Tax (top) or Gag (bottom) proteins by flow cytometry immediately (green line) or 24 h after culture with no (black line), 300 IU/ml (red line) or 3000 IU/ml (blue line) of IFN-α in the presence of IL-2 (30 IU/ml). The closed histogram represents samples stained with isotype controls. The mean fluorescence intensity (MFI) of each histogram was indicated in the bar graphs.

In HUT102 cells, IFN-α suppressed HTLV-1 p19-release but not viral transcription, which is in agreement with previous reports [20].

We also examined the effects of IFN-α in primary ATL cells (Figure 1C). In the absence of IFN-α, intracellular expression of HTLV-1 proteins was spontaneously induced in ATL cells within 24 h after the initiation of culture. IFN-α suppressed the induction of Tax expression in these cells at a concentration of 3000 IU/ml more efficiently than 300 IU/ml. IFN-α also suppressed induction of Gag protein expression but equally at two doses.

Because HTLV-1 mRNA expression was suppressed in ILT-Hod and ILT-#29 cells as well as primary ATL cells following IFN-α treatment, we used these ILTs for further study on the effects of IFN-α at a dose of 3000 IU/ml hereafter.

IFN-α reduced Tax protein expression before reduction of pX mRNA

We next examined the time-course of IFN-α effects on Gag and Tax expression at protein and mRNA levels in ILT-Hod and ILT-#29 cells. Expression of intracellular Tax protein decreased within 1 day after addition of IFN-α to both cell lines. Intracellular Tax expression was maintained at lower levels than the control without IFN-α for at least 8 days (Figure 2A, top panels). Intracellular Gag protein expression in IFN-α-treated cells became lower than untreated cells at later time points (3–8 days), although the levels of viral expression fluctuated during culture (Figure 2A, bottom panels). Expression of HTLV-1 mRNAs in both cell lines were comparable to untreated cells or slightly increased in 1 day after IFN-α treatment, despite the reduction in Tax protein. At later time points (3–8 days), HTLV-1 mRNA levels were significantly decreased (Figure 2B). Thus, in IFN-α-treated ILTs, Tax protein was reduced first without apparent reduction in viral transcription, followed by reduction in viral mRNA and other viral protein expression.

We compared the levels of HTLV-1 proteins and mRNAs at 1 day after IFN-α treatment in these ILTs in several experiments, and confirmed that, at this time point, IFN-α reproducibly suppressed Tax protein levels in both cell lines, whereas the effects of IFN-α were inconsistent on Gag protein levels and not suppressive on HTLV-1 mRNA levels measured by using two different primer sets specific for pX and one for Gag regions (Figure 2C).

We further examined the effects of IFN-α on Tax protein and pX mRNA expression in several other ILT lines derived from ATL and HAM/TSP patients (Figure 2D). Although the suppression rates varied among cell lines, IFN-α suppressed intracellular Tax expression in 6 of 7 ILT cell lines tested in 24 h after IFN-α treatment. In ILT-#294 and HUT102 cells, Tax expression was not suppressed by IFN-α. HTLV-1 mRNA levels were not markedly suppressed or even enhanced in some cell lines in 24 h. Transient enhancement of HTLV-1 mRNA levels were sometimes observed also in ILT-Hod or ILT-#29 in 1 day after IFN-α treatment (Figure 2B, C). The effects of IFN-α on cell growth were limited, with mild reductions observed in some ILT lines after 3–4 days of culture (Figure 2E).

PKR was involved in IFN-α-mediated reduction of Tax protein expression

Since the reduction in intracellular Tax protein levels was induced by IFN-α at an earlier stage than for mRNA in ILT cells, we assumed that some post-transcriptional mechanisms such as PKR-induced translational suppression might be involved. We therefore treated ILT-Hod and ILT-#29 cells with IFN-α in the presence of a chemical PKR-inhibitor or its negative-control (Figure 3A). The otherwise decreased levels of Tax protein in both ILTs in the presence of IFN-α were markedly augmented by the PKR-inhibitor. In both ILTs, the negative-control inhibitor did not alter the Tax protein levels. Interestingly, the PKR-inhibitor increased Tax expression in the absence of IFN-α as well especially in ILT-#29 cells (Figure 3A). The enhancement of Tax expression by PKR-

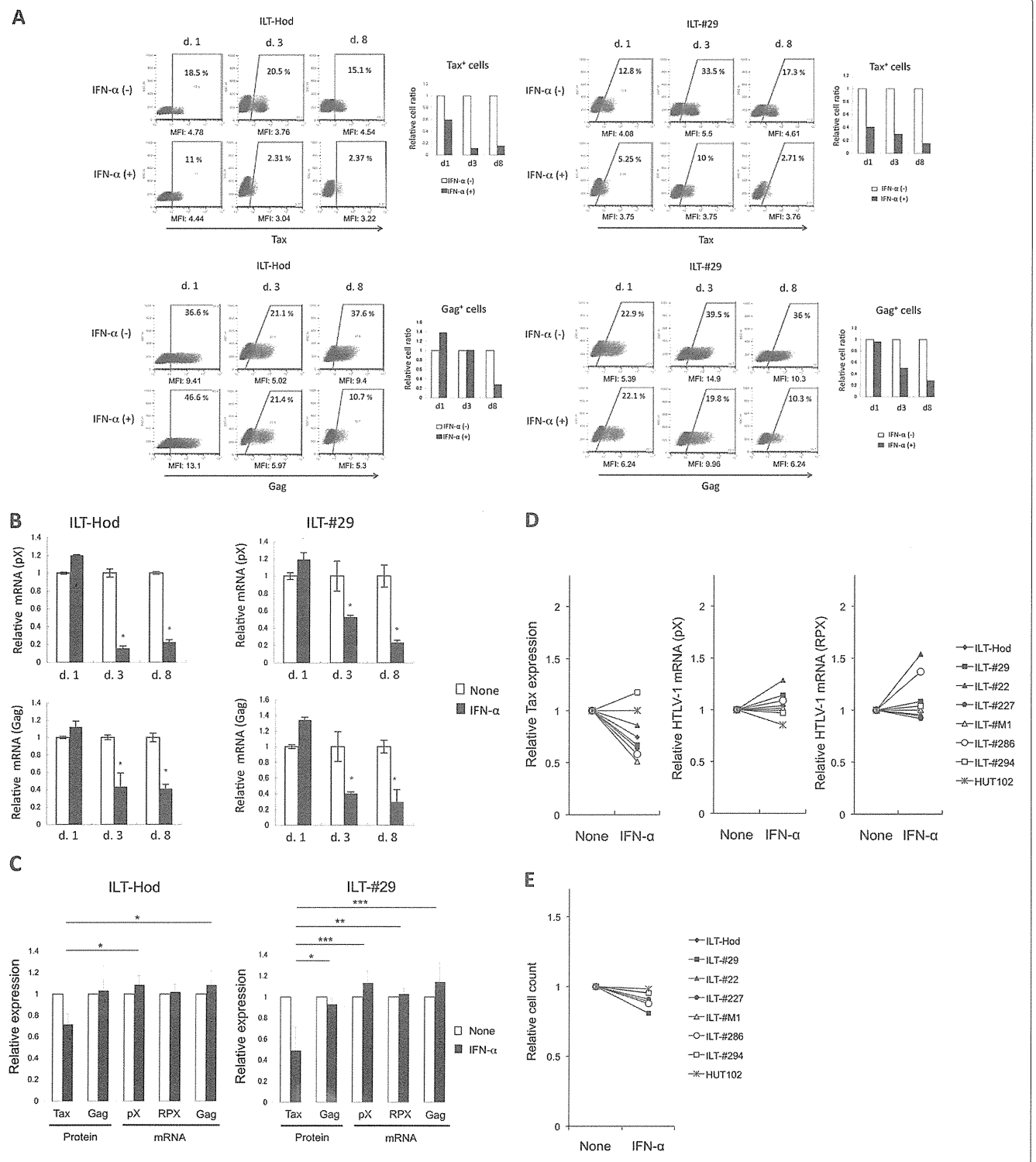

Figure 2 (See legend on next page.)

(See figure on previous page.)
Figure 2 IFN-α suppressed Tax protein expression before an apparent reduction in HTLV-1 mRNA levels. A. The effects of IFN-α (3000 IU/ml) on intracellular Tax (top) and Gag (bottom) protein expression in ILT-Hod (left) and ILT-#29 (right) cells was evaluated by flow cytometry on days 1, 3, and 8 of culture. Cells stained with isotype antibodies served as negative controls. The values inside the dot plots represent percentages of viral protein-expressing cells, and the relative values in IFN-α-treated (closed bar) against untreated (open bar) samples are shown in the bar graph. The MFI value of the total cell population is indicated below the dot plots. **B**. Expression of HTLV-1 mRNA in the same cell samples prepared in A was evaluated by quantitative RT-PCR using pX (top) and Gag (bottom) primers. Results are standardized and presented as relative values of IFN-α-treated (closed bar) against untreated (open bar) samples. The means and SD of duplicate samples are indicated. *$p < 0.05$. **C**. HTLV-1 proteins (Tax and Gag) and HTLV-1 mRNAs expression in ILT-Hod and ILT-#29 cells were measured 24 h after incubation with (closed bar) or without (open bar) IFN-α, and the relative values were indicated as the means and SD of three independent experiments. Three different primer sets (pX, RPX, and Gag) were used to quantify HTLV-1 mRNAs. **D**. Seven ILT lines from various patients and HUT102 were cultured with or without IFN-α for 24 h, and the proportions of Tax positive cells (left) and the HTLV-1 mRNA quantified using pX (middle) and RPX (right) primers were indicated as relative values against the sample without IFN-α. **E**. Various HTLV-1-infected T cell lines shown in D were cultured with or without IFN-α for 3–4 days, and viable cell numbers analyzed by a colorimetric assay were indicated as relative values.

inhibitor was not a result of transcriptional regulation, as HTLV-1 mRNA levels in the cells treated with PKR-inhibitor were comparable to those with control inhibitor (Figure 3B).

We then assessed PKR mRNA expression in these cell lines (Figure 3C). Both ILT lines expressed higher levels of PKR mRNA than HTLV-1-negative Jurkat and MOLT4 cells (Figure 3C). Moreover, IFN-α treatment further increased PKR mRNA expression in ILTs (Figure 3D). These observations indicated that IFN-α suppressed Tax expression at translational level via PKR in ILTs, and also suggested that similar mechanisms might regulate Tax expression in these cells to some extent without exogenous IFN-α.

Effects of IFN-α and AZT on HTLV-1 expression and cell growth

Combination therapy with IFN-α and AZT has been reported to achieve high response rates especially in patients with smoldering and chronic types of ATL, although patients with acute type ATL frequently relapse after therapy [13]. Despite favorable clinical responses, the combination of IFN-α and AZT reportedly shows minimal effects on the viability of HTLV-1-transformed T cells *in vitro* [16]. As we found that IFN-α affected viral expression in ILT-Hod and ILT-#29 cells in our system, we then examined the effects of IFN-α and AZT using these ILTs.

The effects of these drugs on HTLV-1 expression in ILTs was first evaluated. After three days of incubation, when IFN-α-mediated suppression of intracellular Tax protein expression was clearly observed, similar levels of suppression were produced by treatment with the combination of IFN-α and AZT, but not with AZT alone (Figure 4A).

Next, we assessed the effects of these drugs on cell growth. Treatment of IFN-α alone induced mild suppression of cell propagation in one week of culture, while AZT alone did not. The combination of IFN-α and AZT showed stronger suppression of cell growth than IFN-α alone (Figure 4B). The cell cycle analysis indicated that cells treated with IFN-α alone, but not AZT alone, accumulated in the G0/G1 phase. Combined AZT/IFN-α showed a marked increase in apoptotic cell fractions in both ILT-Hod and ILT-#29 cells (Figure 4C). Expression of Ki-67 was also suppressed in these cells by treatment with IFN-α alone or AZT/IFN-α, but not with AZT alone (Figure 4D).

Therefore IFN-α, but not AZT, induced cell-cycle arrest and suppression of viral expression, while AZT combined with IFN-α induced apoptosis in ILT-Hod and ILT-#29 cells.

Suppression of NF-κB activity by IFN-α treatment

NF-κB pathway is constitutively activated and plays a critical role on cell survival in HTLV-1-infected, through Tax-mediated transactivation and other unknown mechanisms [27-29]. We examined the effects of AZT/IFN-α on NF-κB activity using ILT-Hod and ILT-#29 reporter cells stably expressing the NF-κB-responsive element reporter gene. In both cell lines, NF-κB activity was partly but significantly suppressed by IFN-α alone or in combination with AZT, but not with AZT alone (Figure 5A). The reduction in NF-κB activity by IFN-α was also confirmed by the decreases in the mRNA levels of vascular epithelial growth factor (VEGF), one of the NF-κB-regulated genes, in both ILTs treated with IFN-α (Figure 5B).

Involvement of p53-signalling in IFN-α/AZT-mediated apoptosis in ILTs

We finally assessed the effect of IFN-α and AZT on p53 signaling that is known to be impaired in ATL cells [30]. We measured the phosphorylation of p53 in ILTs by flow cytometry (Figure 6A). The levels of phosphorylated p53 clearly increased in both ILTs following treatment with AZT/IFN-α, while IFN-α alone produced minimal effects.

We also evaluated the activity of the p53 pathway by measuring mRNA levels of p53-responsive genes, BAX and p21 (Figure 6B). Levels of BAX and p21 mRNAs were significantly increased in both cell lines treated

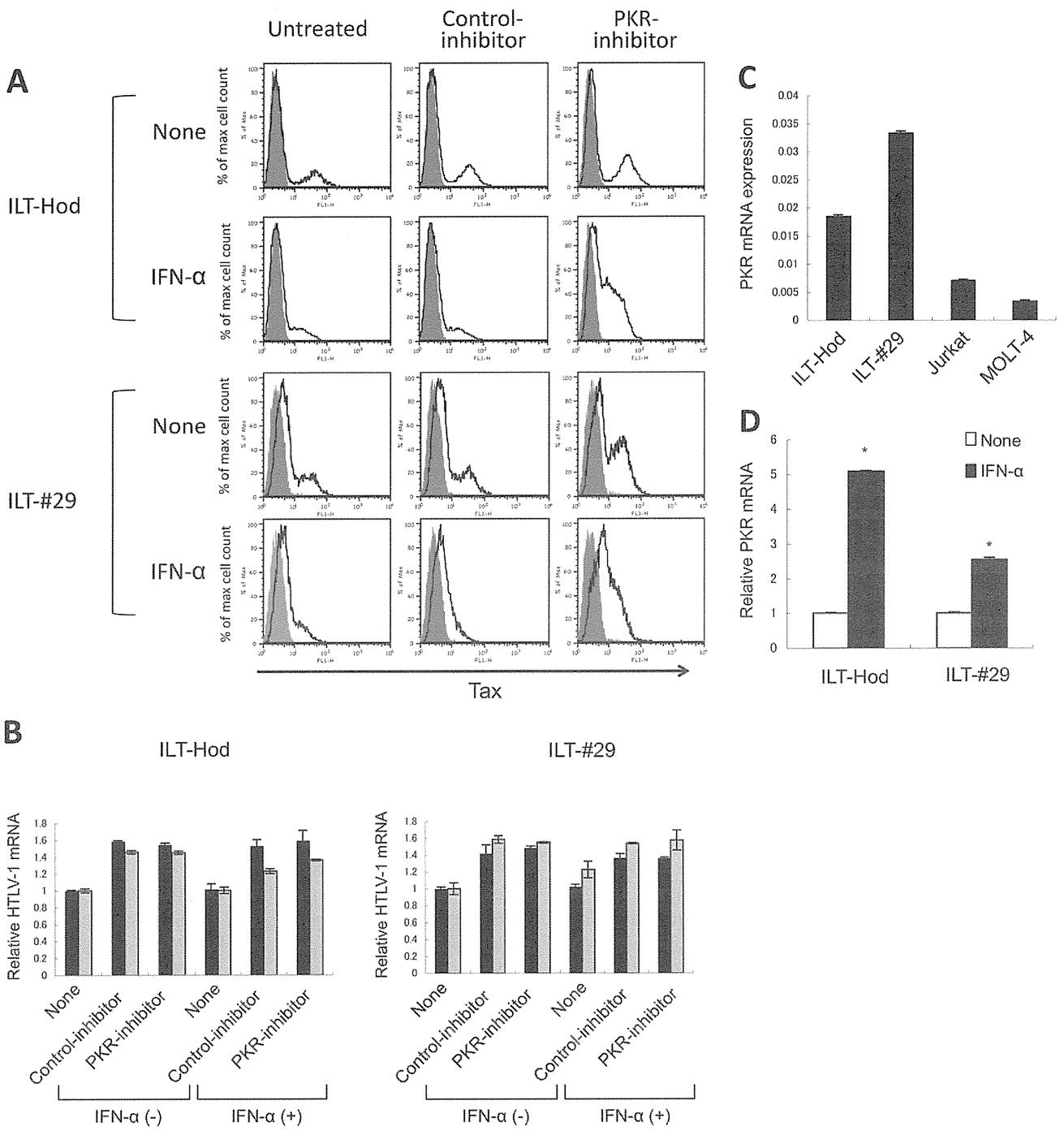

Figure 3 Involvement of PKR in IFN-α-mediated reduction of Tax protein levels in HTLV-1-infected cells. A. ILT-Hod and ILT-#29 cells were incubated with or without the PKR-inhibitor (500 nM) or the negative control-inhibitor (500 nM) for the first 2 h, then further cultured for the next 24 h in the presence or absence of IFN-α (3000 IU/ml) as indicated. Flow cytometry was then performed following stained with anti-Tax (open histogram) and isotype control (closed histogram) antibodies. **B**. HTLV-1 pX mRNAs in the same samples prepared in A were quantified by RT-PCR using two different primer sets (RPX; black bar, and pX; gray bar), standardized to GAPDH mRNAs, and the relative values were indicated as the means and SD of duplicate samples. **C**. PKR mRNAs in ILT-Hod, ILT-#29, and HTLV-1-negative Jurkat and MOLT4 cells were quantified by RT-PCR, standardized to GAPDH mRNA and indicated as the means and SD of duplicate samples. **D**. PKR mRNAs in ILT-Hod and ILT-#29 cells were quantified 24 h after culture in the absence (open bar) or presence (closed bar) of IFN-α (3000 IU/ml), and the relative values are indicated as the means and SD of duplicate samples. *$p < 0.05$.

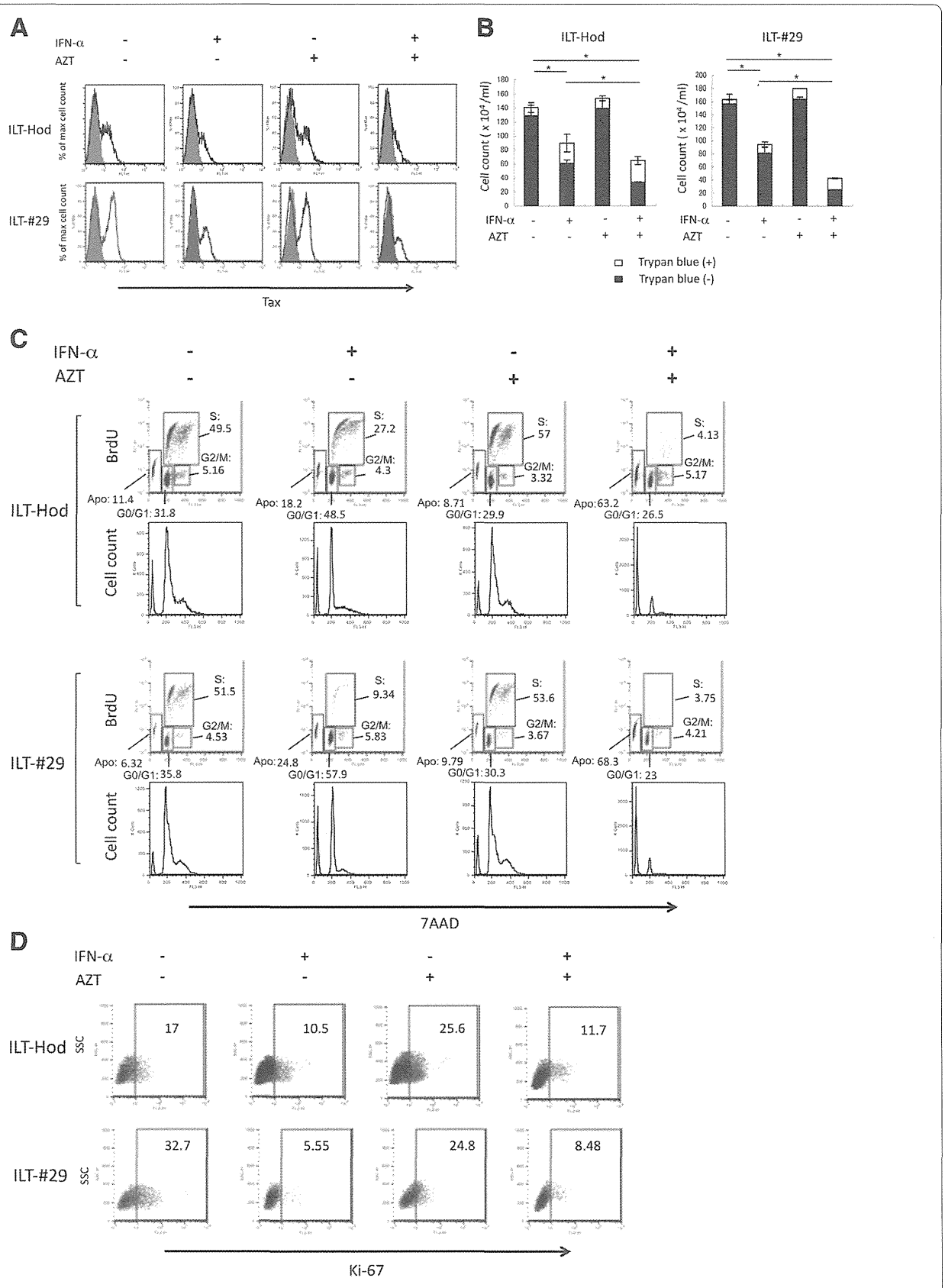

Figure 4 (See legend on next page.)

(See figure on previous page.)
Figure 4 Effects of IFN-α and AZT on HTLV-1 expression and cell growth of HTLV-1 infected cells. ILT-Hod and ILT-#29 cells (10^6/ml) were cultured in the absence or presence of IFN-α (3000 IU/ml) and/or AZT (10 μM) as indicated, and HTLV-1 expression (**A**), cell growth (**B**), cell cycle (**C**), and Ki-67 expression (**D**) in the cells were evaluated. **A**. Expression of intracellular Tax protein 3 days after the initiation of culture was evaluated by flow cytometry following stained with anti-Tax (open histogram) and isotype control (closed histogram) antibodies. **B**. ILT-Hod and ILT-#29 cells were similarly treated with IFN-α and/or AZT, and maintained with addition of equal volumes of fresh medium without IFN-α or AZT on the day 1 and 3, then viable (closed bar) and non-viable (open bar) cell numbers in cultures were evaluated by trypan blue exclusion on the day 8. *$p < 0.05$. **C**. ILT-Hod and ILT-#29 cells similarly treated with IFN-α and/or AZT were subjected to cell cycle analysis on the day 8. Cultures were treated with BrdU (10 μM) for the last 24 h of culture then permeabilized and incubated with a FITC-labeled mouse anti-BrdU antibody and 7AAD. Cells that are 7AAD-negative can be considered apoptotic (Apo). BrdU-negative and 7AAD-intermediate positive cells are in the G0/G1 phase. BrdU-positive and 7AAD-positive cells are in the S phase. BrdU-negative and 7AAD-highly positive cells are in the G2/M phase. The values in the dot plots indicate the proportion of the cells (%) in each phase. **D**. ILT-Hod and ILT-#29 cells similarly treated with IFN-α and/or AZT were analyzed for intracellular Ki-67 expression by flow cytometry on the day 8. The values in the dot plots indicate the proportion of Ki-67-positive cells (%).

with the combination of AZT and IFN-α. IFN-α alone slightly enhanced BAX and p21 mRNA levels in ILT-#29 cells but not in ILT-Hod cells. Effects of AZT alone were marginal in both cell lines.

The use of a p53-inhibitor partly reduced the apoptotic fraction in AZT/IFN-α-treated ILTs compared with those without inhibitor (Figure 6C). The effects of the p53-inhibitor were limited, however, probably because of a short half-life of the inhibitor.

These observations indicated that the combination of AZT and IFN-α effectively activated p53 pathway that was invoved in cell apoptosis in ILT-Hod and ILT-#29 cells.

Discussion

In the present study, we have demonstrated that IFN-α suppressed HTLV-1 gene expression in infected cells. This is consistent with our previous findings, which indicated that stromal cells suppressed viral expression in HTLV-

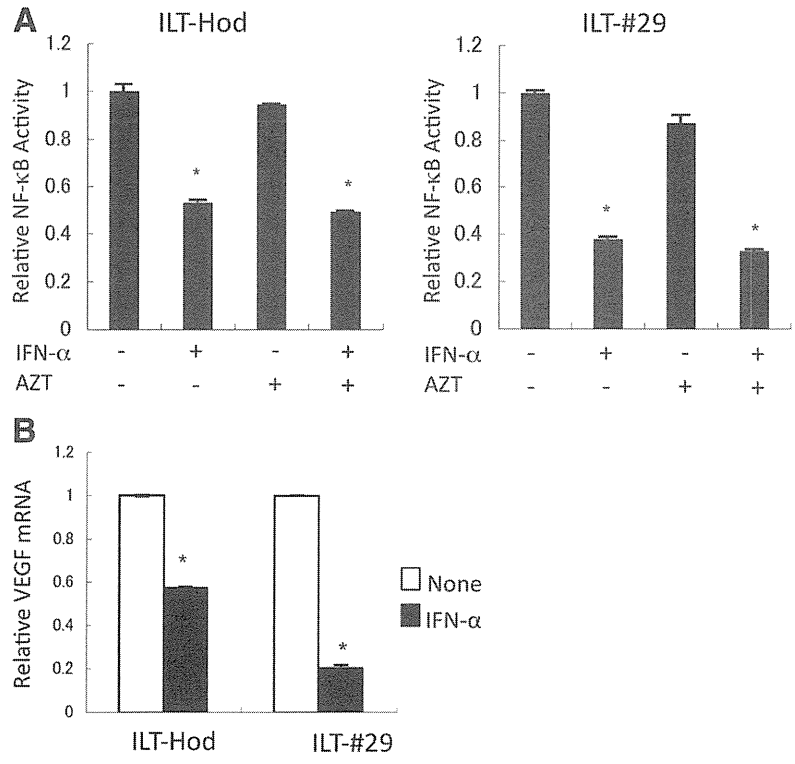

Figure 5 Suppression of NF-κB activity by IFN-α in HTLV-1-infected cells. A. ILT-Hod and ILT-#29 cells that were infected with lentiviral vectors containing reporter gene for the NF-κB responsive element and the TK-promoter several weeks before, were treated with or without IFN-α (3000 IU/ml) and/or AZT (10 μM) for 4 days as indicated. Luciferase activities were measured, and relative NF-κB activities normalized to TK-promoter activities were indicated as means and SD of duplicate samples. *$p < 0.05$. **B**. The levels of mRNA of VEGF, a NF-κB-regulated gene, in ILT-Hod and ILT-#29 cells 3 days after incubation with (closed bar) or without (open bar) IFN-α (3000 IU/ml) were quantified by RT-PCR and standardized to GAPDH mRNA. The relative values are indicated as means and SD of duplicate samples. *$p < 0.05$.

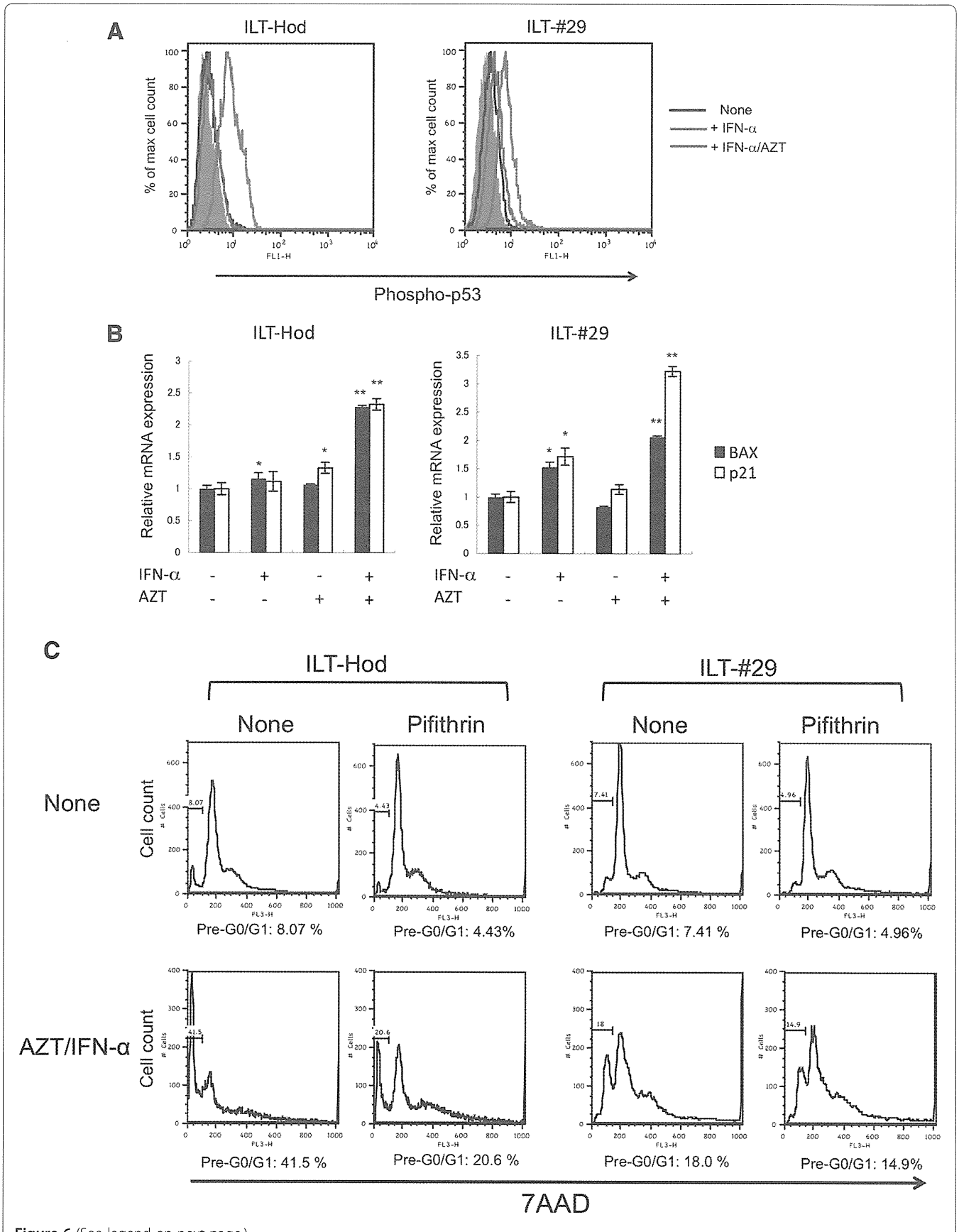

Figure 6 (See legend on next page.)

(See figure on previous page.)
Figure 6 Induction of p53-signaling by IFN-α and AZT in HTLV-1-infected cells. A. Intracellular phosphorylated p53 levels in ILT-Hod and ILT-#29 cells were evaluated by flow cytomertry 3 and 4 days after incubation, respectively, in the absence (black line) or presence of IFN-α (3000 IU/ml) alone (blue line), or IFN-α/AZT (10 μM) (red line). The closed histograms indicate cells stained with control antibody. **B**. ILT-Hod and ILT-#29 were treated with IFN-α and/or AZT for 4 days and mRNA expression of BAX (closed bar) and p21 (open bar) was evaluated by quantitative RT-PCR. Results are standardized with the copy number of GAPDH mRNA, and the relative values are indicated as means and SD of duplicate samples. *$p < 0.05$, **$p \leq 0.01$. **C**. ILT-Hod and ILT-#29 cells were cultured with or without IFN-α/AZT in the presence or absence of a p53-inhibitor (Pifithrin-α p-Nitro Cyclic, 1 μM) for 3 days and 5 days, respectively, then the cells were analyzed for the cell cycle by flow cytometry following 7AAD-staining. The proportions of apoptotic cell fractions (pre G0/G1) were indicated below each histogram.

1-infected T-cells via type I IFN when co-cultured [26]. However, these findings conflict with most other reports [16,20-22]. Differences among opposing findings can be attributed to the differences in the HTLV-1-infected cells used. It has been reported that type I IFNs inhibit HTLV-1 p19 release but not viral gene expression in HTLV-1-transformed cells [20]. This was true for HUT102 cells also in the present study, but not for ILT cells (Figure 1B). One of the differences between HUT102 and ILTs is the levels of Tax protein, which is present at much higher levels in HUT102 than ILTs. Because expression of HTLV-1 proteins is barely detectable *in vivo*, we hypothesize that HTLV-1-infected cells in vivo might retain susceptibility to IFNs similarly to ILTs rather than HUT102. Indeed, IFN-α suppressed HTLV-1 gene expression in primary ATL cells that was induced in a short-term culture *in vitro* (Figure 1C).

Reduction in intracellular Tax protein levels preceded transcriptional suppression of viral mRNA in ILTs when treated with IFN-α (Figure 2), indicating involvement of some post-transcriptional mechanisms such as decreased protein translation and/or increased proteolysis [19]. In this study, we found that PKR was involved in IFN-α–mediated Tax suppression (Figure 3). PKR is a ubiquitously expressed serine/threonine kinase, induced by IFNs and activated by double-stranded RNA to phosphorylate its substrates. These substrates include the alpha subunit of translation initiating factor eIF-2, thereby resulting in inhibition of protein synthesis [31-33]. Since the Tax protein positively regulates HTLV-1 transcription through interaction with the HTLV-1 long terminal repeat (LTR) [34,35], it would be reasonable that suppression of HTLV-1 transcription followed the reduction in Tax protein levels. However, the PKR-mediated translational control alone does not explain why Tax protein decreased earlier than Gag protein following IFN-α treatment in ILTs (Figure 2A, C), suggesting the involvement of additional mechanisms to produce preferential reduction of Tax.

It is intriguing that ILTs often show a histogram with two phases in the flow cytometric analysis for HTLV-1 proteins especially for Tax, despite the fact that all the ILT cells are infected with HTLV-1. This suggests that Tax protein levels in ILTs fluctuate between detectable and undetectable levels during culture. For the HUT102 cells, there was always a single peak of Tax-positive cells (Figure 1A). Nevertheless, the HTLV-1 transcription levels are comparable in ILTs and HUT102 (Figure 1A). In addition, the PKR inhibitor abrogated IFN-α-mediated suppression of Tax expression in ILTs without changing mRNA levels (Figure 3A, B). We also found that addition of the PKR inhibitor enhanced Tax expression in the absence of exogenous IFN-α especially for ILT-#29 cells (Figure 3A). Moreover, PKR expression was spontaneously increased in ILTs and further augmented by IFN-α (Figure 3C, D). These findings suggest that Tax protein synthesis might be spontaneously regulated by PKR to some extent in these cells, although it is unclear what activates PKR. If highly structured transcripts from HTLV-1 themselves were the activators of PKR, they might also activate other molecules such as 2', 5'-oligoadenylate synthetase that can also suppress viral expression. HTLV-1 expression might be regulated by such negative feedback systems to maintain equilibrium levels in ILT cells. Further studies will be required to understand the entire system regulating HTLV-1 expression in infected cells.

We noticed some differences with respect to the effects of IFN-α on HTLV-1 gene expression, p19 release, and cell growth in various HTLV-1-infected cell lines, which cannot be fully explained simply by the different levels of Tax expression in these cells, implying the presence of multiple mechanisms resisting against signaling pathways downstream of the IFN-αβ receptor. The mechanisms other than Tax determining IFN susceptibility remain to be clarified.

NF-κB is activated in HTLV-1-infected cells and plays a critical role in survival of these cells [36]. Our results indicate that IFN-α suppressed both viral expression and NF-κB activity; AZT did not affect either of these. Because Tax is a strong activator of NF-κB, IFN-α-mediated reduction of Tax protein levels likely results in IFN-α-mediated suppression of NF-κB (Figure 5A). However, the suppression of NF-κB activity by IFN-α in ILTs was partial. This is presumably attributed to the incompleteness of IFN-α-mediated suppression of Tax expression, and also to the presence of Tax-independent mechanisms for NF-κB activation in these cells.

Although IFN-α inhibited cell growth in ILTs, it was not cytocidal. Cell cycle analysis revealed that IFN-α